

INTERSTELLAR GLYCINE

YI-JEHNG KUAN,^{1,2} STEVEN B. CHARNLEY,³ HUI-CHUN HUANG,¹ WEI-LING TSENG,¹ AND ZBIGNIEW KISIEL⁴

Received 2002 November 15; accepted 2003 April 1

ABSTRACT

We have searched for interstellar conformer I glycine ($\text{NH}_2\text{CH}_2\text{COOH}$), the simplest amino acid, in the hot molecular cores Sgr B2(N-LMH), Orion KL, and W51 e1/e2. An improved search strategy for intrinsically weak molecular lines, involving multisource observations, has been developed and implemented. In total, 82 spectral frequency bands, in the millimeter-wave region, were observed over a 4 yr period; 27 glycine lines were detected in 19 different spectral bands in one or more sources. The rotational temperatures derived from “rotation diagrams” are 75^{+29}_{-16} K for Sgr B2(N-LMH), 141^{+76}_{-37} K for Orion KL, and 121^{+71}_{-32} K for W51 e1/e2. The total column densities inferred are $4.16^{+3.22}_{-1.82} \times 10^{14} \text{ cm}^{-2}$ for Sgr B2, $4.37^{+1.79}_{-1.27} \times 10^{14} \text{ cm}^{-2}$ for Orion, and $2.09^{+1.22}_{-0.77} \times 10^{14} \text{ cm}^{-2}$ for W51. Production of interstellar glycine by both gas-phase ion-molecule reactions and by ultraviolet photolysis of molecular ices is briefly discussed. The discovery of interstellar glycine strengthens the thesis that interstellar organic molecules could have played a pivotal role in the prebiotic chemistry of the early Earth.

Subject headings: astrobiology — ISM: abundances —

ISM: individual (Orion Kleinmann-Low, Sagittarius B2(N-LMH), W51 e1/e2) —

ISM: molecules — line: identification — radio lines: ISM

1. INTRODUCTION

Interstellar clouds, similar to that from which the solar system formed, contain many organic molecules (e.g., Ehrenfreund & Charnley 2000). Early investigations of prebiotic chemistry attempted to produce those biomolecules that are the building blocks of living organisms by the energetic processing of the simple molecules (e.g., water, methane, ammonia, formaldehyde) thought to have dominated the atmosphere of the early Earth (Miller 1957). The known interstellar aldehydes, acids, ketones, and sugars have important functions in terrestrial biochemistry and could also have been important in prebiotic synthesis. Large quantities of the organic material necessary to initiate prebiotic chemistry could have been delivered to the early Earth by the impacts of comets and asteroids (e.g., Oró 1961; Chyba et al. 1990; Delsemme 1993). The volatile molecular inventory of comets shows a striking similarity to that of dense molecular clouds (e.g., Ehrenfreund & Charnley 2000; Kuan et al. 2003a), and simple interstellar organics may have also acted as the precursors of the more complex organics found in meteorites, formed through aqueous processing on their parent bodies (e.g., Cronin & Chang 1993). Hence, comparison with the composition of comets and meteorites suggests that one could in principle trace the origin of Earth’s prebiotic chemistry back to the parent interstellar cloud. If more complex organics, such as amino acids, exist in interstellar space (Ehrenfreund et al. 2001c), then they may have “jump started” prebiotic chemistry on the early Earth.

Among the biologically important molecules, glycine ($\text{NH}_2\text{CH}_2\text{COOH}$) is the simplest amino acid. Astronomical searches for glycine commenced as soon as laboratory spectra became available (Suenram & Lovas 1978, 1980; Brown et al. 1978) and have continued up to the present (Brown et al. 1979; Hollis et al. 1980; Snyder et al. 1983; Berulis et al. 1985; Guélin & Cernicharo 1989; Miao et al. 1994; Combes, Nguyen-Q-Rieu, & Wlodarczak 1996; Ceccarelli et al. 2000; Helo 2003; Hunt et al. 2003; Kuan et al. 2003b, 2003c). Glycine has several structural conformers (e.g., Császár 1992), and astronomical searches have focused on the lowest-energy conformer I and the higher-energy conformer II, which has a much larger dipole moment (Lovas et al. 1995). The observational difficulties associated with searching for large interstellar molecules in line-rich, compact, hot molecular cores (HMCs), and glycine in particular, have been summarized by Snyder (1997). These include the intrinsic weakness of the lines due to the large molecular partition functions, and the contamination of the target transitions by emission from the many other molecules (“interlopers”) present in the HMCs and their accompanying, extended molecular envelopes.

To overcome the problems of line weakness and interlopers, searches based on “deep” integrations of carefully selected, favorable transitions at higher frequencies are crucial, as is the avoidance of known high-density spectral regions. Observations of transitions of higher frequencies sample the warmer, denser regions in the cloud, and this reduces the interloping emission from surrounding cold material. Furthermore, line intensities generally increase in proportion to ν^3 , and so observing at higher frequencies helps to prevail over the low-lying interlopers.

The interloper problem may be partially resolved by interferometric observations; these can filter out the unwanted extended emission that presumably comes from more spatially distributed simple molecules. However, observations of $\text{C}_2\text{H}_5\text{OH}$ in Orion KL by Ohishi et al. (1995) found that ethanol emission is rather extended

¹ Department of Earth Sciences, National Taiwan Normal University, 88 Sec. 4, Ting-Chou Road, Taipei 116, Taiwan, Republic of China.

² Academia Sinica, Institute of Astronomy and Astrophysics, P.O. Box 23-141, Taipei 106, Taiwan, Republic of China.

³ Space Science Division, MS 245-3, NASA Ames Research Center, Moffett Field, CA 94035.

⁴ Institute of Physics, Polish Academy of Sciences, Al. Lotnikow 32/46, 02-668 Warsaw, Poland.

($\sim 30''$); methanol (CH_3OH) and glycolaldehyde ($\text{CH}_2\text{OH-CHO}$) were also observed to have a spatial scale of $\geq 60''$ toward Sgr B2(N-LMH) (Halfen, Apponi, & Ziurys 2001; Hollis et al. 2001). In particular, a large fraction of the glycolaldehyde emission was found to originate from the lower density envelope surrounding the Sgr B2(N-LMH) hot core (Hollis et al. 2001).

We have therefore conducted an extensive and thorough search for conformer I glycine using the former NRAO Kitt Peak 12 m telescope⁵ toward three HMCs in regions of ongoing massive star formation: Sgr B2(N-LMH), Orion KL, and W51 e1/e2. In this paper we present the observational data and briefly discuss the broad astrochemical and astrobiological implications of the discovery of interstellar glycine.

2. OBSERVATIONS

The observations of glycine were carried out during nine observing seasons with the NRAO 12 m telescope. These spanned 4 years, from 1997 November to 2001 March, and covered the frequency ranges 200–265 GHz ($\lambda \sim 1.3$ mm), 130–170 GHz (~ 2 mm), and occasionally, in less favorable weather conditions, 90–116 GHz (~ 3 mm). The dual-channel 3 mm–hi, 2 mm, and 1 mm–lo SIS mixer receivers were used in single-sideband mode. The sideband rejection was ≥ 20 dB. Chopper-vane calibration corrected for atmospheric extinction and telescope losses was used; the resultant data are on the T_R^* scale. For most of our observations, the 256-channel filter bank spectrometers of 1 and 2 MHz resolution were used in parallel mode (2×128); filter banks of 1 MHz and 500 kHz resolution were adopted for all observations taken from 2000 December to 2001 March. The half-power beamwidths are $\sim 30''$, $\sim 45''$, and $\sim 60''$ at 1.3, 2, and 3 mm, respectively. The main-beam efficiencies varied from 95% at 90 GHz to $\sim 49\%$ at 240 GHz. Data were obtained in the position-switching mode with offset $20'$ west in azimuth. The 12 m data were reduced using the NRAO Unipops software.

2.1. Multisource Search

We have searched in three HMCs: Sgr B2(N-LMH) [$\alpha(\text{B1950.0}) = 17^{\text{h}}44^{\text{m}}10^{\text{s}}20$, $\delta(\text{B1950.0}) = -28^{\circ}21'15''0$], Orion KL at the compact ridge [$\alpha(\text{B1950.0}) = 5^{\text{h}}32^{\text{m}}47^{\text{s}}00$, $\delta(\text{B1950.0}) = -5^{\circ}24'30''0$], and W51 e1/e2 [$\alpha(\text{B1950.0}) = 19^{\text{h}}21^{\text{m}}26^{\text{s}}30$, $\delta(\text{B1950.0}) = +14^{\circ}24'39''0$]. The LSR velocities adopted for the search were 64.0, 8.0, and 60.0 km s^{-1} for Sgr B2(N-LMH), Orion KL, and W51 e1/e2, respectively. Limited by the available local sidereal time ranges of each source and constrained by the observing schedules, very often certain glycine transitions could be observed only in one or two of the sources. Overall, more transitions in Orion KL were observed because Orion has the longest up-time, whereas the up-times of Sgr B2 and W51 are shorter and basically overlap.

Among the three target sources, Sgr B2(N-LMH) is, in principle, the best source in which to search for large organic molecules, because of its rich chemistry and stron-

ger line intensities. Although strong glycine line intensities are desirable for giving the higher signal-to-noise ratios needed for detection, all other nonglycine molecular lines also become stronger and wider in Sgr B2. Of the spectral lines characteristic of each source, those detected in Sgr B2 have the largest average velocity dispersions, and it is easy for broad, strong lines from numerous abundant molecules to partially or completely obscure any nearby weak glycine lines. These issues are representative of the major challenges for the identification of complex molecules like glycine; they forced us to discard many putative glycine lines in Sgr B2. Moreover, because of its complicated dynamical and chemical nature, the velocity field of Sgr B2(N-LMH) is not uniquely defined. The V_{LSR} of known lines can vary from 58 to 75 km s^{-1} (Kuan & Snyder 1994, 1996; Snyder 1997; Mehringer et al. 1997; Nummelin et al. 2000; Turner & Apponi 2001; Hollis et al. 2002). This rather large LSR velocity uncertainty also creates a significant problem for the identification of weak glycine lines in Sgr B2 (N-LMH), especially since a weak-line forest already exists.

In contrast, Orion KL has a much better defined velocity field and exhibits generally modest line widths. Within the 12 m beam, the V_{LSR} of the compact ridge is known to be ~ 8 km s^{-1} , and ~ 5 km s^{-1} for the hot core. A velocity field extending from ~ 3 to 11 km s^{-1} is considered reasonable in Orion KL (Blake et al. 1987; Liu, Mehringer, & Snyder 2001; Lee, Cho, & Lee 2001). Although its chemistry appears less rich compared to Sgr B2(N-LMH), Orion KL seems to be a good candidate source for detection. Nevertheless, spectra taken near the hot core in Orion often include emission from simpler molecules, excited in the adjacent warm, shocked environment. As a result of this, there is an increased probability of partial or complete smearing of nearby targeted glycine lines.

W51 e1/e2 has the best defined velocity field, with V_{LSR} between 55 and 61 km s^{-1} (Zhang, Ho, & Ohashi 1998; Liu et al. 2001). Furthermore, since spectral lines in W51 e1/e2 have the narrowest average line profiles, the line-blending problem should be least severe, yielding a significant advantage for line identifications in W51. However, judging from the low line densities found in overall observed spectra, W51 appears to be the least chemically active source among the three sources searched. This suggests that a lower glycine column density, and hence weaker line intensities, are to be expected in W51. We were forced to discard many potential glycine lines in W51 simply because their peak intensities fall below the 3σ detection criterion.

An obvious consequence of a multisource search is that it could be extremely time consuming, particularly for intrinsically weak-line molecules. However, by carefully comparing the spectral line patterns and velocity information from the individual spectra of each source, we are able to recognize and accurately identify most of the spectral line features, which appear in each of the spectral frequency bands searched. The velocity-field discrepancy in an individual source is therefore self-determined and self-resolved when a consistent velocity pattern can be decided among various spectral features present in all three sources (see § 3.2). A multisource search is therefore one of the most effective ways to distinguish glycine lines from interlopers that result from the weak-line forest. As a result of this multisource test, quite a number of potential glycine lines were excluded. A multisource check is also a good method for identifying and rejecting those weak “lines” that are false detections

⁵ The National Radio Astronomy Observatory is a facility of the National Science Foundation, operated under cooperative agreement by Associated Universities, Inc. This telescope is now operated by Arizona Radio Observatory (ARO) of the University of Arizona.

arising from rare, accidental variations in the noise and gain within the system.

2.2. Spectral Frequency Bands Searched

Dedicated glycine observations were conducted in 1998 November 12–19 and 1999 March 28–April 1. These were supplemented by searches for serendipitous detections of glycine lines in similar quality data, taken during several 12 m searches for other large organics in the 1997–2001 period. The data analysis presented here employed a glycine frequency list adopted from the JPL catalog (Pickett et al. 1998). This line list is calculated on the basis of the data obtained from Suenram & Lovas (1980) and Lovas et al. (1995), with rotational quantum numbers $J \leq 41$ and frequencies up to the submillimeter region. The uncertainties of the calculated frequencies are in general larger toward higher J and K transitions, which tend to carry larger centrifugal distortion contributions. Nevertheless, the frequencies of all astronomically detected transitions are in excellent agreement with JPL predictions. To minimize system noise, deep integrations were performed in all spectral bands observed. Typically, an integration time of ≥ 5 hr was achieved; integration times of 10 hr or more were not unusual. Frequency shifting of ± 4 MHz (± 2 MHz at 500 kHz resolution) with respect to the rest frequency was executed as a common practice during observations, in order to neutralize the effect of potential low-level gain variations in the filter banks.

The dedicated observations were conducted with 23 different frequency bands tuned at 1 and 2 mm wavelengths. The bandwidths are of 128 MHz for 1 MHz spectral resolution and 256 MHz for 2 MHz resolution. All spectral bands contain glycine transitions carefully selected as being highly favorable for the avoidance of line-blending from adjacent strong lines and interlopers, because of other molecules known to be present in star-forming clouds. Of the 23 bands searched, 14 glycine “lines”⁶ are detected in 11 bands. The remaining glycine lines searched are either blended with unidentified lines (U-lines) or with neighboring lines of known molecules with large line widths. Since these 14 lines are not detected in all three sources (see § 2.1), more glycine lines are necessary for a definite detection. We therefore sought chance detections of glycine in other data taken during 1997–2001.

Data taken in 1997 November and December and in 1998 January and April included 27 spectral bands that could possibly contain strong glycine transitions; three glycine lines in two bands are clearly identified. A further 21 frequency bands were searched in the data observed in 1999 November and 2000 March–June; four glycine lines⁷ are detected in four different bands. Observations carried out from 2000 December to 2001 March were also examined since these included 11 spectral bands expected to contain reasonably favored glycine transitions; seven glycine lines, including a four-line quadruplet, are detected in two separate bands. In summary, of the 82 spectral bands searched, 27 glycine lines in 19 separate frequency bands are detected in one or more HMCs.

⁶ Each “line” may include multiple glycine transitions that are blended into one unresolved, single spectral feature.

⁷ One of the four lines was also detected in a different source in the earlier run between 1997 November and 1998 April.

3. RESULTS

3.1. Glycine Transitions Detected

Table 1 shows all the transitions detected in 27 separate spectral lines. These glycine lines are numbered with increasing frequency (col. [1]). No glycine line at 3 mm is detected. Glycine transitions (col. [3]) in each line are listed with increasing rest frequency (col. [2]) except in lines 10, 19, 20, and 24, where the specific leading frequencies are the ones that were tuned to in the actual observations. The dipole moments of conformer I glycine are $\mu_a = 0.911(3)$ and $\mu_b = 0.607(5)$ D (Lovas et al. 1995); hence, a -type transitions are slightly more favored over b -type transitions, as can be easily seen from the tabulated line strengths (col. [5]). The last column (col. [6]) lists all the likely interlopers that might be partially blended with the detected glycine lines. The information of these interlopers is given in “molecule/transition/frequency (MHz)” format and is self-explanatory. However, many of the potential *known* interlopers are estimated to have negligibly weak line intensities, due either to being unfavorable transitions or to very low expected abundances; these include rare isotopomers and molecules more usually found only in dark clouds or circumstellar envelopes. These trivial interlopers are noted as “unlikely.” Interloping spectral features that have no known molecular counterparts are denoted as unidentified U-lines. In a very few cases, the partially blended spectral features are seen only in a certain source, and special remarks are given next to these interlopers. To exclude the possibility of any potential interlopers coming in from the other sideband, image sidebands of all detected glycine lines were carefully checked for strong lines. No strong lines in image sidebands of intensities greater than 0.5 K were found to come close to the detected glycine lines.

Table 2 lists the important observed physical parameters of all the glycine lines. Column (1) gives the line numbers, which correspond to the line numbers shown in column (1) of Table 1. The glycine lines are separated into three sources according to their actual detections. These sources are indicated in the table section headings, along with the rotational excitation temperatures and total column densities as derived from “rotation diagrams” constructed for each source (see § 3.3). Some of the glycine lines are only observed in one or two sources but not in all for various reasons, such as availability of observing time, confusion from nearby broad emission lines, detection limit, and discrepancy in velocity field (see § 2.1, and § 3.2 below). In total, 13 glycine lines are detected in Sgr B2, 15 in Orion, and 16 in W51. Among the 27 lines, three lines are observed in all three sources, two lines are found in both Sgr B2 and Orion, four lines in Sgr B2 and W51, and another five in the Orion-W51 pair. The peak LSR velocities (col. [2]) are not Gaussian-fitted since weak molecular lines are known to be non-Gaussian (Turner 1989). The velocity uncertainty simply reflects the spectral resolution employed and does not include effects that might be introduced by possible pointing error, hence toward a slightly different velocity field, and/or by partial line-blending in some cases, which makes the precise determination of peak velocities harder to achieve. Column (3) gives the measured peak antenna temperatures in T_R^* ; the temperature uncertainty indicates the rms noise level of the spectrum and does not include possible pointing errors. Uncertainties in the integrated line intensities (col. [4]) are attributed to both the indeterminate extent of the

TABLE 1
THE MOLECULAR LINE PARAMETERS OF THE GLYCINE TRANSITIONS DETECTED

Line ^a (1)	Rest Frequency ^b (2)	Transitions (3)	E_u ^c (4)	S_{ul} ^d (5)	Potential Interlopers Partially Blended with Glycine ^e (6)
1.....	130346.589(0.095)	21 _{1,20} -20 _{2,19}	72.3	16.7	U-130349
2.....	130354.185(0.095)	21 _{2,20} -20 _{2,19}	72.3	20.5	HCOOCH ₃ /51 _{8,43} -50 _{10,40} <i>A</i> /130351.8 (unlikely) ^f U-130349
3.....	130360.703(0.095)	21 _{1,20} -20 _{1,19}	72.3	20.5	U-130358 (in Sgr B2 and Orion)
4.....	130368.298(0.095)	21 _{2,20} -20 _{1,19}	72.3	16.7	<i>a</i> -CH ₂ CHOH/22 _{6,17} -23 _{5,18} /130373.0 (in Sgr B2 and W51)
5.....	131423.488(0.105)	19 _{3,16} -18 _{3,15}	67.6	18.1	U-131420; C ₂ H ₅ CN/88 _{5,83} -87 _{7,80} /131424.8 (unlikely) ^f
6.....	142225.352(0.223)	12 _{5,8} -11 _{4,7}	34.0	4.6	HCOOCH ₃ /16 _{1,15} -16 _{0,16} /142229.0 CC ¹³ CCH/15-14 <i>F</i> = 15-14/142225.3 (unlikely) ^g
7.....	142300.826(0.141)	21 _{3,18} -20 _{3,17}	81.0	20.0	H ₂ ¹³ CO/18 _{2,16} -19 _{0,19} /142299.1 (unlikely) ^h (CH ₃) ₂ CO/25 _{25,0} -25 _{24,1} <i>EA</i> /142299.5 (unlikely) ^f CH ₂ CDCN/15 _{2,13} -14 _{2,12} /142304.6
8.....	144841.834(0.084)	21 _{9,12} -20 _{9,11}	102.9	17.2	<i>c</i> -C ¹³ CCH ₂ /18 _{15,4} -18 _{14,5} /144839.1 DCN/2-1/144827
9.....	144847.127(0.108)	21 _{5,17} -20 _{5,16}	84.8	19.7	
10.....	147813.913(0.152)	24 _{1,23} -23 _{1,22}	92.7	23.5	HO ¹³ CO ⁺ /27 _{1,27} -28 _{0,28} /147814.8 (unlikely) ^g
	147811.758(0.152)	24 _{1,23} -23 _{2,22}	92.7	19.7	C ₂ H ₅ OH/21 _{4,17} -20 _{5,16} <i>v</i> = 1/147815.8
	147812.896(0.152)	24 _{2,23} -23 _{2,22}	92.7	23.5	H ₂ CNH/14 _{4,11} -15 _{3,12} /147817.5
	147814.763(0.158)	22 _{3,19} -21 _{3,18}	88.0	21.0	<i>s</i> -CH ₂ CHOH/42 _{4,39} -41 _{5,36} /147818.9 (unlikely) ^f
	147815.051(0.152)	24 _{2,23} -23 _{1,22}	92.7	19.7	
11.....	148267.851(0.278)	25 _{0,25} -24 _{1,24}	94.0	23.6	U-148263
	148267.860(0.278)	25 _{1,25} -24 _{1,24}	94.0	24.8	<i>c</i> -C ₃ D/3 _{1,2} -2 _{1,1} <i>F</i> = 4-3/148263.1 (unlikely) ^{h,i}
	148267.868(0.278)	25 _{0,25} -24 _{0,24}	94.0	24.8	<i>c</i> -C ₃ D/3 _{1,2} -2 _{1,1} <i>F</i> = 3-2/148267.3 (unlikely) ^{h,i}
	148267.876(0.278)	25 _{1,25} -24 _{0,24}	94.0	23.6	
12.....	150909.783(0.083)	22 _{12,11} -21 _{12,10}	130.8	15.5	CH ₂ DCH ₂ CN/4 _{3,1} -3 _{2,2} /150910.3 (unlikely) ^h
	150909.784(0.083)	22 _{12,10} -21 _{12,9}	130.8	15.5	C ₂ H ₅ OH/20 _{3,18} -20 _{2,18} <i>v</i> = 1-0/150915.9
13.....	160153.458(0.133)	23 _{6,18} -22 _{6,17}	103.5	21.4	U-160144 CH ₂ CDCN/16 _{5,11} -17 _{4,14} /160146.1 (unlikely) ^h C ₂ H ₅ CN/62 _{9,53} -63 _{8,56} /160146.6 (unlikely) ^f C ₂ H ₅ CN/35 _{6,29} -36 _{5,32} <i>v</i> = 2/160154.1 (unlikely) ^f
14.....	164851.302(0.197)	26 _{2,24} -25 _{3,23}	113.7	18.8	U-164850
15.....	164861.611(0.197)	26 _{3,24} -25 _{3,23}	113.7	25.2	
16.....	164870.010(0.197)	26 _{2,24} -25 _{2,23}	113.7	25.2	U-164868 (CH ₃) ₂ CO/31 _{12,19} -31 _{11,20} <i>EE</i> /164870.1 (unlikely) ^f (CH ₃) ₂ CO/31 _{13,19} -31 _{12,20} <i>EE</i> /164870.1 (unlikely) ^f
17.....	164880.319(0.198)	26 _{3,24} -25 _{2,23}	113.7	18.8	U-164878 CH ₃ C ₃ N/40 ₁₅ -39 ₁₅ /164880.1 (unlikely) ^f
18.....	164886.186(0.115)	24 _{12,13} -23 _{12,12}	146.4	18.0	C ₂ H ₅ CN/48 _{4,45} -47 _{5,42} /164883.8
	164886.189(0.115)	24 _{12,12} -23 _{12,11}	146.4	18.0	HCC ¹³ CCCN/62-61/164885.7 (unlikely) ^g
19.....	165270.602(0.233)	27 _{1,26} -26 _{1,25}	115.7	26.5	HCOOCH ₃ /9 _{3,7} -8 _{2,6} /165276.0
	165270.289(0.233)	27 _{1,26} -26 _{2,25}	115.7	22.7	<i>c</i> - ¹³ CCCH/7 _{5,3} -7 _{3,4} /165277 (unlikely) ^h
	165270.452(0.233)	27 _{2,26} -26 _{2,25}	115.7	26.5	U-165268 (in W51 only)
	165270.765(0.233)	27 _{2,26} -26 _{1,25}	115.7	22.7	
20.....	205559.895(0.406)	33 _{3,31} -32 _{3,30}	176.8	32.2	CH ₂ CDCN/3 _{3,1} -2 _{2,0} /205560.7 (unlikely) ^{h,j}
	205559.761(0.406)	33 _{2,31} -32 _{3,30}	176.8	25.7	HCOOCH ₃ /46 _{29,17} -47 _{28,19} <i>E</i> /205560.7 (unlikely) ^f
	205560.014(0.406)	33 _{2,31} -32 _{2,30}	176.8	32.2	CH ₂ CDCN/22 _{16,6} -21 _{16,5} /205565.5
	205560.149(0.406)	33 _{3,31} -32 _{2,30}	176.8	25.6	CH ₂ CDCN/22 _{16,7} -21 _{16,6} /205565.5
21.....	206468.023(0.847)	35 _{0,35} -34 _{0,34}	180.5	34.8	C ₂ H ₅ CN/23 _{18,5} -22 _{18,4} /206457.2
	206468.023(0.847)	35 _{0,35} -34 _{1,34}	180.5	33.6	C ₂ H ₅ CN/23 _{18,6} -22 _{18,5} /206457.2
	206468.023(0.847)	35 _{1,35} -34 _{0,34}	180.5	33.6	
	206468.023(0.847)	35 _{1,35} -34 _{1,34}	180.5	34.8	
22.....	212286.362(0.928)	36 _{0,36} -35 _{0,35}	190.7	35.8	NH ₂ CHO/10 _{6,5} -9 _{6,4} ,10 _{6,4} -9 _{6,3} /212277.0
	212286.362(0.928)	36 _{0,36} -35 _{1,35}	190.7	34.6	<i>c</i> -CC ¹³ CH/4 _{1,3} -3 _{1,2} <i>F</i> = 4-3/212286.0 (unlikely) ^h
	212286.362(0.928)	36 _{1,36} -35 _{0,35}	190.7	34.6	C ₃ D/40 ₀ -40 ₁ /212287.3 (unlikely) ^h
	212286.362(0.928)	36 _{1,36} -35 _{1,35}	190.7	35.8	C ₂ H ₅ CN/39 _{3,37} -39 _{1,38} /212289.9 (unlikely) ^f
23.....	223003.319(0.540)	36 _{2,34} -35 _{3,33}	208.2	28.9	<i>s</i> -CH ₂ CHOH/4 _{2,3} -3 _{1,2} /222996.8
	223003.339(0.540)	36 _{3,34} -35 _{3,33}	208.2	35.2	C ₂ H ₅ CN/43 _{2,41} -43 _{2,42} <i>v</i> = 2/223005.0 (unlikely) ^f
	223003.357(0.540)	36 _{2,34} -35 _{2,33}	208.2	35.2	CH ₃ CCCN/54 ₄ -53 ₄ /223006.8 (unlikely) ^{g,k}
	223003.376(0.540)	36 _{3,34} -35 _{2,33}	208.2	28.9	U-223008
24.....	228419.333(0.550)	36 _{3,33} -35 _{3,32}	216.3	34.9	<i>c</i> -C ₃ HD/11 _{8,4} -11 _{6,5} /228415.7 (unlikely) ^h
	228418.243(0.550)	36 _{3,33} -35 _{4,32}	216.3	25.9	<i>c</i> -C ₃ H ₂ /22 _{16,7} -22 _{15,8} <i>v</i> = 1/228417.7 (unlikely) ^f
	228418.836(0.550)	36 _{4,33} -35 _{4,32}	216.3	34.9	C ₂ H ₅ CN/24 _{11,13} -23 _{11,12} <i>v</i> = 2/228417.9 (unlikely) ^f
	228419.927(0.550)	36 _{4,33} -35 _{3,32}	216.3	25.9	C ₂ H ₅ CN/24 _{11,14} -23 _{11,13} <i>v</i> = 2/228417.9 (unlikely) ^f U-228425 (in Sgr B2 and W51 only)

TABLE 1—Continued

Line ^a (1)	Rest Frequency ^b (2)	Transitions (3)	E_u ^c (4)	S_{ul} ^d (5)	Potential Interlopers Partially Blended with Glycine ^e (6)
25.....	230348.069(0.629)	33 _{6,27} –32 _{6,26}	202.5	31.3	O ¹³ CS/19–18/230317.5 (broad; in Orion only) C ₂ H ₃ CN/84 _{6,79} –83 _{7,76} $v = 1$ /230349.8 (unlikely) ^f CH ₃ OH/22 ₄ –21 ₅ /230368.7 (broad; in Orion only)
26.....	240899.571(0.954)	40 _{1,39} –39 _{2,38}	244.2	35.8	U-240894; C ₃ H/39 ₁ –38 ₀ /240895.7 (unlikely) ^f
	240899.571(0.954)	40 _{1,39} –39 _{1,38}	244.2	39.5	C ₂ H ₃ CN/39 _{3,37} –40 _{1,40} /240902.6 (unlikely) ^{f,i}
	240899.571(0.954)	40 _{2,39} –39 _{1,38}	244.2	35.8	H ¹³ COOH/31 _{3,28} –31 _{3,29} /240903.9 (unlikely; ^f Orion?)
	240899.571(0.954)	40 _{2,39} –39 _{2,38}	244.2	39.5	C ₇ H/8–7/240901 (unlikely) ^g
27.....	241372.658(1.410)	41 _{0,41} –40 _{0,40}	245.9	40.8	c - ¹³ CCCH/8 _{3,6} –8 _{1,7} $F = 9$ –9/241370.0 (unlikely) ^h
	241372.658(1.410)	41 _{1,41} –40 _{0,40}	245.9	39.6	c - ¹³ CCCH/8 _{3,6} –8 _{1,7} $F = 8$ –8/241374.3 (unlikely) ^h
	241372.658(1.410)	41 _{1,41} –40 _{1,40}	245.9	40.8	S ¹⁷ O/6 _{5,7} –5 _{4,7} /241370.6 (unlikely) ^h
	241372.658(1.410)	41 _{0,41} –40 _{1,40}	245.9	39.6	C ₂ H ₃ CN/19 _{3,17} –20 _{0,20} /241365.4 (unlikely) ^f U-241367

^a Each line may include multiple glycine transitions that are blended into one unresolved, single spectral-line feature.

^b In MHz. Values in parentheses are the 1σ uncertainties.

^c Upper energy levels, in K.

^d Line strengths.

^e “Unlikely” indicates that the intensity of the presumed interloper is estimated to be negligibly weak. This could be due either to the interloping line being an unfavorable transition, because of its extremely low line strength and/or unreasonably high excitation, or to the exceedingly low expected abundance of the interloper, such as in the case of a rare isotopomer or a circumstellar or dark-cloud molecule. Additional remarks are given where necessary.

^f Very unfavored transitions.

^g Rare isotopomers or circumstellar or dark-cloud molecules.

^h A combination of a rare isotopic species and unfavored transitions.

ⁱ The 9_{3,6}–9_{3,7} transition of c -C₃H (see Figs. 1*d* and 1*f*) is expected to be ≥ 20 times stronger than its 3_{1,2}–2_{1,1} transition in LTE. However, no c -C₃H was detected in Orion KL (Fig. 1*e*). The c -C₃D line in Orion considered here would be negligible if the [D/H] abundance ratio were also taken into account.

^j In LTE, the 3_{3,1}–2_{2,0} transition of CH₂CDCN at 205,560.7 MHz is estimated to be more than 20 times weaker than the combined intensity of 22_{16,7}–21_{16,6} and 22_{16,6}–21_{16,5} transitions at 205,565.5 MHz. Also, in Sgr B2, the 205,560 MHz glycine line is at $V_{\text{LSR}} \simeq 67.0$ km s⁻¹, while the CH₂CDCN line at 205,565.5 MHz is at $\simeq 64.0$ km s⁻¹; and in W51, the glycine line is at $\simeq 58.6$ km s⁻¹, while CH₂CDCN at 205,565.5 MHz is at $\simeq 55.2$ km s⁻¹ (see Figs. 2*c* and 2*d*).

^k Of the seven CH₃C₃N transitions, 54_{*}–53_{*} with * = 0–6, that fall into the spectral band, transitions 54₀–53₀, 54₂–53₂, and 54₅–53₅ are at or below the 1σ level, ~ 10 mK; the remaining four are blended. Note that the glycine line is now at 223,000.6 MHz ($V_{\text{LSR}} = 67.3$ km s⁻¹; see Fig. 2*e*).

^l Large rest-frequency uncertainty, ± 9.8 MHz; 240,897.2 MHz from JPL catalog.

line-blending, namely, the equivalent line widths, and the measurement errors of T_R^* .

Many candidate transitions of glycine lie in the spectral bands searched. A glycine detection rests on the fact that there should be no interloper-free lines absent from the spectra that would exhibit detectable intensities equal to or above 3σ . Table 3 gives a full accounting of all glycine transitions that we searched for; this includes transitions that fell into our spectral bands but that we failed to detect. Column (1) gives the rest frequency of each glycine transition (col. [2]) with increasing frequency. Line strengths and the lower energy levels of listed glycine transitions are given in columns (3) and (4), respectively. To simplify the table, glycine transitions with intrinsic line strengths smaller than 1.0 are excluded unless they are self-blended with other glycine transitions possessing line strengths greater than 1.0. Redundant glycine transitions, those that were observed in the same source more than once in different spectral bands, are listed only once. The exact reasons for identifying these lines as nondetections are commented upon in columns (5)–(7) for each of the target sources: Sgr B2(N-LMH) (col. [5]), Orion KL (col. [6]), and W51 e1/e2 (col. [7]).

In most cases, a nondetection results either from line-blending with one or more interlopers or from the measured line intensity falling below 3σ . Interlopers that are severely blended with the candidate glycine lines, thus making a secure identification impossible, are listed in columns (5)–(7) in Table 3 and are shown in the format “molecule/

frequency (MHz).” Interloping transitions of molecular species that, for various reasons (e.g., see footnotes f, g, and h of Table 1), have negligible expected line intensities are not included since, practically, they have no influence on our judgement of whether or not a line is detected. Because their line intensities and line widths are source dependent, interlopers listed in each source may not be identical. For glycine candidate lines that are free from any apparent interloper with reasonable line intensity, the expected line intensity $T_R^*(\text{exp})$ and the rms noise σ of the spectrum are thus given (in mK). The $T_R^*(\text{exp})$ is predicted based on the actual fits of individual rotation diagrams of each source, namely, the T_{rot} and the total derived column density (see § 3.3), along with the mean equivalent line width obtained by averaging over all detected glycine lines in the corresponding source. One glycine candidate line in Sgr B2,⁸ five in Orion,⁹ and one in W51¹⁰ are predicted to be stronger than 3σ and hence should have been detected; however, these lines all suffered from poor weather conditions or various system problems during the observations. Other comments given in columns (5), (6), and (7) are self-explanatory.

⁸ Transitions 19_{9,11}–18_{9,10} and 19_{9,10}–18_{9,9} at 130,717 MHz.

⁹ Transitions 22_{12,10}–21_{12,9} and 22_{12,11}–21_{12,10} at 150,909 MHz; 27_{*26}–26_{*25}, * = 1, 2, at 165,270 MHz; 33_{*31}–32_{*30}, * = 2, 3, at 205,560 MHz; 36_{2,34}–35_{3,33}, * = 2, 3, at 223,003 MHz; and 41_{*41}–40_{*40}, * = 0, 1, at 241,372 MHz.

¹⁰ Transitions 24_{12,13}–23_{12,12} and 24_{12,12}–23_{12,11} at 164,886 MHz.

TABLE 2

MEASURED PHYSICAL PARAMETERS OF THE GLYCINE LINES DETECTED

Line (1)	V_{LSR}^a (km s ⁻¹) (2)	T_R^* (mK) (3)	$W_K^b \pm \text{Uncertainty}$ (10 ⁻² K km s ⁻¹) (4)
Sgr B2(N-LMH) ($T_{\text{rot}} = 75_{-16}^{+29}$ K, $N_{\text{tot}} = 4.16_{-1.82}^{+3.22} \times 10^{14}$ cm ⁻²) ^c			
1.....	66.3 ± 1.2	26.0 ± 5.9	8.97 ± 3.56
2.....	66.3 ± 1.2	30.0 ± 5.9	17.20 ± 5.87
6.....	64.0 ± 5.6	22.0 ± 2.0	12.40 ± 4.61
7.....	64.0 ± 2.1	38.0 ± 2.2	48.10 ± 18.86
10.....	64.0 ± 1.0	20.0 ± 5.0	12.18 ± 4.08
12.....	68.0 ± 2.7	18.0 ± 2.5	14.33 ± 4.71
19.....	64.8 ± 0.9	60.0 ± 4.6	20.00 ± 3.33
20.....	67.0 ± 0.7	95.0 ± 11.9	41.61 ± 12.15
21.....	66.0 ± 1.9	210.0 ± 8.9	81.2 ± 18.70
22.....	66.0 ± 0.7	58.0 ± 15.6	16.36 ± 6.45
23.....	67.3 ± 1.8	40.0 ± 10.5	21.44 ± 8.33
24.....	65.0 ± 1.3	70.0 ± 7.6	36.68 ± 13.16
26.....	63.2 ± 0.6	94.0 ± 11.0	34.97 ± 7.01
Orion KL ($T_{\text{rot}} = 141_{-37}^{+76}$ K, $N_{\text{tot}} = 4.37_{-1.27}^{+1.79} \times 10^{14}$ cm ⁻²) ^c			
1.....	8.0 ± 3.1	9.0 ± 2.0	6.21 ± 2.42
5.....	8.5 ± 1.1	15.0 ± 4.1	17.10 ± 5.58
6.....	7.8 ± 2.8	5.2 ± 1.4	1.90 ± 0.95
8.....	5.0 ± 2.8	20.9 ± 3.8	17.27 ± 5.31
9.....	8.0 ± 1.4	17.9 ± 5.2	11.98 ± 3.85
11.....	5.0 ± 2.0	11.0 ± 2.1	15.15 ± 4.34
14.....	7.5 ± 1.2	21.2 ± 4.5	5.79 ± 2.44
15.....	7.5 ± 1.2	25.0 ± 4.5	13.65 ± 4.21
16.....	7.5 ± 1.2	20.0 ± 4.5	9.10 ± 3.50
17.....	7.5 ± 1.2	17.7 ± 4.5	4.83 ± 2.16
18.....	7.5 ± 1.2	21.6 ± 4.5	11.79 ± 4.17
21.....	7.3 ± 0.7	230.0 ± 10.0	133.40 ± 14.15
24.....	4.9 ± 3.5	40.0 ± 2.0	41.92 ± 10.00
25.....	8.0 ± 3.5	26.0 ± 3.9	27.00 ± 7.51
26.....	5.0 ± 1.7	35.0 ± 7.2	21.70 ± 8.82
W51 e1/e2 ($T_{\text{rot}} = 121_{-32}^{+71}$ K, $N_{\text{tot}} = 2.09_{-0.77}^{+1.22} \times 10^{14}$ cm ⁻²) ^c			
3.....	60.0 ± 3.1	7.5 ± 2.2	4.31 ± 1.72
4.....	60.0 ± 3.1	6.4 ± 2.1	3.11 ± 2.02
5.....	60.0 ± 3.0	15.0 ± 4.0	8.21 ± 2.60
7.....	60.0 ± 2.8	6.6 ± 2.8	4.18 ± 2.14
8.....	56.0 ± 2.8	20.7 ± 2.9	12.85 ± 3.97
9.....	60.0 ± 1.4	15.5 ± 4.2	10.22 ± 3.97
12.....	58.0 ± 2.0	8.0 ± 1.5	8.40 ± 2.40
13.....	60.0 ± 2.5	37.0 ± 4.1	10.47 ± 4.32
15.....	60.0 ± 1.2	14.6 ± 4.0	7.97 ± 2.50
19.....	58.2 ± 2.4	8.0 ± 2.1	4.50 ± 1.75
20.....	58.6 ± 3.9	17.0 ± 4.1	14.89 ± 6.14
21.....	60.5 ± 0.7	65.0 ± 9.7	37.7 ± 8.01
24.....	57.0 ± 1.8	40.0 ± 5.1	10.48 ± 2.65
25.....	58.7 ± 3.5	19.0 ± 6.0	24.70 ± 8.70
26.....	57.0 ± 1.7	17.0 ± 5.5	6.32 ± 2.74
27.....	57.0 ± 1.7	26.0 ± 6.4	16.12 ± 6.44

^a The LSR velocity of the spectral line peak.^b The integrated line intensity.^c The rotational excitation temperatures and total column densities are derived from linear least-squares fits of the individual rotation diagrams (see Fig. 4).

Sample glycine spectra are shown in Figures 1, 2, and 3. Figure 1 displays six spectra of two different glycine lines in all three sources: line 21 (at 206,468 MHz) in Sgr B2, Orion, and W51 (Figs. 1a, 1b, and 1c, respectively), and likewise line 26 (at 240,899 MHz) in Figures 1d, 1e, and 1f. Eight

glycine spectra at six different frequencies are presented in Figure 2; of the eight spectra, three are of Sgr B2(N-LMH), three of W51 e1/e2, and two of Orion KL. Figures 2a and 2b exhibit spectra of Sgr B2 and W51, respectively, at 165,270 MHz (line 19), similarly at 205,560 MHz (line 20) in Figures 2c and 2d. The remaining four spectra shown in Figures 2e–2h are glycine lines at 223,003 MHz (line 23 in Sgr B2), 131,423 MHz (line 5 in Orion), 228,419 MHz (line 24 in Orion), and 241,372 MHz (line 27 in W51), respectively. Figure 3 shows the glycine spectrum of the quadruplet lines at 164.8 GHz (lines 14, 15, 16, and 17), plus the line at 164,886 MHz (line 18) in Orion.

3.2. Velocity Field and Multisource Check

The peak velocities of glycine lines in Sgr B2(N-LMH) display a slightly larger spread when compared to those in the other two sources (Table 2). This may be partly due to broader intrinsic line widths in Sgr B2, which lead to more interloping blends with glycine lines (see Fig. 1). In contrast, the velocity ranges are more confined and better determined in Orion KL and W51 e1/e2. A major advantage of multi-source spectral comparisons is that sharper line profiles in one source (e.g., W51) can unveil the two-component nature of broad line-profiles that would be otherwise overlooked in another source (typically Sgr B2 or Orion). For example, the glycine line at 131,423.4 MHz (line 5) shown in Figure 2f is partially blended with a weak U-line at 131,420 MHz; this is not obvious in the Orion spectrum but is clearly revealed in the W51 spectrum. Such information is therefore useful in better determining the integrated line intensities.

The difficulty in assigning a consistent and correct LSR velocity to a particular molecular species in a hot core and hence identifying it can be demonstrated in Figure 1. The peak LSR velocities, in km s⁻¹, of the known molecular emission found in Sgr B2(N-LMH) in the frequency band between 206,418 and 206,518 MHz as shown in Figure 1a are ~65.1 for C₂H₅CN at 24_{1,24}–23_{1,23} but ~60.7 at 23_{18,5}–22_{18,4} and 23_{18,6}–22_{18,5}; ~64.0 for HCOOCH₃ at both 14_{8,7}–14_{7,8} E and 14_{8,6}–14_{7,7} E; ~66.8 for C₆H at 75₂–74₂; and ~67.0 for HCOOCH₃ at 14_{8,6}–14_{7,7} A. The LSR velocity in Sgr B2 ranges from ~60.7 to ~67.0 km s⁻¹ in one single spectrum alone. Similarly, in Orion KL we found (Fig. 1b) ~9.1 for C₂H₅CN at 24_{1,24}–23_{1,23} but ~5.5 at 23_{18,5}–22_{18,4} and 23_{18,6}–22_{18,5}; ~8.0 for HCOOCH₃ at 14_{8,7}–14_{7,8} E and ~7.4 at 14_{8,6}–14_{7,7} E; and ~7.5 for C₆H at 75₂–74₂ and ~6.5 for HCOOCH₃ at 14_{8,6}–14_{7,7} A. In this single spectrum of Orion KL, the LSR velocity varies from ~5.5 to ~9.1 km s⁻¹. It is apparent that even in the same frequency band, at an identical spatial position and with an equal beam size, different molecules or the same molecule at different transitions have various LSR velocities. As an example, the spectral feature at 206,496.8 MHz in Sgr B2 (Fig. 1a) can be attributed to either the 75₂–74₂ transition of C₆H at 206,498.7 MHz or the 50₄–49₄ transition of CH₃CCCN at 206,495.5 MHz. By comparison with the same spectral feature in Orion, now at 206,499.1 MHz (Fig. 1b), the candidate molecule CH₃CCCN can therefore be eliminated. Careful comparisons of the spectral velocity patterns between the three HMCs are therefore crucial for the correct identification of weak glycine lines; such a pattern check is a powerful way to avoid false identifications.

Applying LSR velocities respectively of 64, 8, and 60 km s⁻¹ to our actual observations of Sgr B2, Orion, and W51,

TABLE 3
SUMMARY OF ALL GLYCINE TRANSITIONS OBSERVED

Rest Frequency (MHz) (1)	Transitions (2)	S_{ul} (3)	E_l (cm ⁻¹) (4)	Sgr B2(N-LMH) (5)	Orion KL (6)	W51 e1/e2 (7)
79711.612.....	13 _{2,11} -12 _{3,10}	4.8	19.8	U-79709	S ¹⁸ O/79716.3	U-79709
86374.884.....	21 _{4,18} -21 _{3,19}	8.2	53.5	Not observed	Not observed	C ₂ H ₅ OH/86375.4 DNO/86374.3
88097.566.....	15 _{7,8} -15 _{6,9}	7.4	35.8	$T_R^*(\text{exp}) = 5.2$ $\sigma = 4.6$	Not observed	Not observed
88624.551.....	14 _{7,7} -14 _{6,8}	6.6	32.3	HNCO/88624.4 HNO/88624.3 HCN/88631.8	Not observed	Not observed
88704.010.....	13 _{12,2} -12 _{12,1}	1.9	51.0	Not observed	(CH ₃) ₂ O/88709.1	(CH ₃) ₂ O/88709.1
88704.010.....	13 _{12,1} -12 _{12,0}	1.9	51.0			
88711.844.....	14 _{7,8} -14 _{6,9}	6.6	32.3	Not observed	(CH ₃) ₂ O/88709.1 C ₂ H ₅ CN/88713.2	(CH ₃) ₂ O/88709.1 C ₂ H ₅ CN/88713.2
88755.840.....	13 _{11,3} -12 _{11,2}	3.7	45.7	Not observed	C ₂ H ₅ CN/88752.8, 88758.5	C ₂ H ₅ CN/88752.8, 88758.5
88755.840.....	13 _{11,2} -12 _{11,1}	3.7	45.7			
88913.450.....	13 _{9,4} -12 _{9,3}	6.8	36.5	Not observed	C ₂ H ₅ C ¹⁵ N/88914.2	C ₂ H ₅ C ¹⁵ N/88914.2
88913.450.....	13 _{9,5} -12 _{9,4}	6.8	36.5			
89026.498.....	13 _{7,6} -13 _{6,7}	5.9	29.1	Not observed	C ₂ H ₅ CN/89026 ^a	C ₂ H ₅ CN/89026 ^a
93953.151.....	25 _{4,21} -25 _{3,22}	11.0	77.1	Not observed	$T_R^*(\text{exp}) = 5.7$ $\sigma = 4.4$	Not observed
102552.810.....	24 _{4,21} -24 _{3,22}	8.2	68.2	Not observed	CH ₃ CCH/102547.9 DNCO/102552 (CH ₃) ₂ CO/102555 CH ₂ (OH)CHO/102549.7	Observed in fog
102574.002.....	31 _{8,24} -31 _{7,25}	18.4	126.0	Not observed	U-102576 CH ₂ (OH)CHO/102572.9	Observed in fog
102628.043.....	15 _{10,6} -14 _{10,5}	8.3	47.0	Not observed	CH ₂ CDCN/102627.1	Observed in fog
102628.044.....	15 _{10,5} -14 _{10,4}	8.3	47.0		C ₂ H ₃ CN/102627.9 C ₂ H ₅ OH/102625.6 HNC ¹⁸ O/102628.4 CH ₂ CDCN/102633.2	
106638.818.....	27 _{4,23} -27 _{3,24}	11.0	88.7	C ₂ H ₃ CN/106641.4 HCOOCH ₃ /106632.8	C ₂ H ₃ CN/106641.4 HCOOCH ₃ /106632.8	C ₂ H ₃ CN/106641.4 HCOOCH ₃ /106632.8
111177.322.....	33 _{6,27} -33 _{6,28}	1.4	137.1	HCOOCH ₃ /111171.6	U-111179	U-111179
112250.700.....	17 _{3,15} -16 _{3,14}	16.2	32.8	Not observed	CH ₃ CHO/112248.7 CH ₂ (OH)CHO/112247.9 C ₂ H ₅ OH/112251.5 CH ₃ CHO/112253.6 HCCCHO/112255.3 HCOOCH ₃ /112256.5	CH ₃ CHO/112248.7 CH ₂ (OH)CHO/112247.9 C ₂ H ₅ OH/112251.5 CH ₃ CHO/112253.6 HCCCHO/112255.3 HCOOCH ₃ /112256.5
130247.662.....	19 _{10,9} -19 _{9,10}	8.4	62.1	SiO/130268.6	SiO/130268.6	SiO/130268.6
130248.384.....	19 _{10,10} -19 _{9,11}	8.4	62.1	C ₂ H ₅ OH/130246.2 C ₂ H ₃ CN/130244.7	C ₂ H ₅ OH/130246.2 C ₂ H ₃ CN/130244.7	C ₂ H ₅ OH/130246.2 C ₂ H ₃ CN/130244.7
130346.589.....	21 _{1,20} -20 _{2,19}	16.7	45.9	Detected	Detected	U-130349
130354.185.....	21 _{2,20} -20 _{2,19}	20.5	45.9	Detected	U-130349	U-130349
130360.703.....	21 _{1,20} -20 _{1,19}	20.5	45.9	U-130358	U-130358	Detected

TABLE 3—Continued

Rest Frequency (MHz) (1)	Transitions (2)	S_{ul} (3)	E_l (cm ⁻¹) (4)	Sgr B2(N-LMH) (5)	Orion KL (6)	W51 e1/e2 (7)
130368.298.....	21 _{2,20} –20 _{1,19}	16.7	45.9	CH ₂ CHOH/130373.0	CH ₂ CHOH/130373.0	Detected
130430.156.....	19 _{10,10} –18 _{10,9}	13.8	62.1	NH ₂ CN/130422.2	NH ₂ CN/130422.2	NH ₂ CN/130422.2
130430.172.....	19 _{10,9} –18 _{10,8}	13.8	62.1	<i>c</i> -C ₃ HD/130422.5 C ₂ H ₅ OH/130419.7	<i>c</i> -C ₃ HD/130422.5 C ₂ H ₅ OH/130419.7	<i>c</i> -C ₃ HD/130422.5 C ₂ H ₅ OH/130419.7
130476.103.....	20 _{3,18} –19 _{2,17}	12.6	44.6	HCOOCH ₃ /130475.7	HCOOCH ₃ /130475.7	HCOOCH ₃ /130475.7
130716.645.....	19 _{9,11} –18 _{9,10}	14.8	57.8	T_R^* (exp) = 22.0 ^b	T_R^* (exp) = 12.7 ^b	T_R^* (exp) = 6.7 ^b
130717.120.....	19 _{9,10} –18 _{9,9}	14.8	57.8	$\sigma = 3.7$	$\sigma = 7.9$	$\sigma = 5.3$
130777.052.....	17 _{10,7} –17 _{9,8}	6.9	53.6	C ₂ H ₃ CN/130776.5	C ₂ H ₃ CN/130776.5	C ₂ H ₃ CN/130776.5
130777.141.....	17 _{10,8} –17 _{9,9}	6.9	53.6			
130787.662.....	8 _{6,3} –7 _{5,2}	5.5	12.2	C ₂ H ₃ NC/130786.6	C ₂ H ₃ NC/130786.6	C ₂ H ₃ NC/130786.6
130788.859.....	8 _{6,2} –7 _{5,3}	5.5	12.2	CH ₂ CDCN/130787.9 HCOOCH ₃ /130788.4	CH ₂ CDCN/130787.9 HCOOCH ₃ /130788.4	CH ₂ CDCN/130787.9 HCOOCH ₃ /130788.4
130802.946.....	22 _{0,22} –21 _{0,21}	21.8	46.7	SO ¹⁸ O/130811.9	SO ¹⁸ O/130811.9	SO ¹⁸ O/130811.9
130802.815.....	22 _{0,22} –21 _{1,21}	20.6	46.7	U-130795	U-130795	U-130795
130802.881.....	22 _{1,22} –21 _{1,21}	21.8	46.7			
130803.013.....	22 _{1,22} –21 _{0,21}	20.6	46.7			
131149.321.....	15 _{10,5} –15 _{9,6}	5.3	46.1	Not observed	C ₂ H ₃ CN/131151.8	Not observed
131149.329.....	15 _{10,6} –15 _{9,7}	5.3	46.1		HNCO/131151.3 C ₂ H ₃ CN/131147.2	
131196.492.....	20 _{3,17} –19 _{4,16}	8.9	47.2	Not observed	³³ SO ₂ /131195.8 ³³ SO ₂ /131186.7	Not observed
131288.303.....	14 _{10,4} –14 _{9,5}	4.5	42.6	Not observed	C ₂ H ₅ OH/131289.7	SO ₂ /131274.9
131288.305.....	14 _{10,5} –14 _{9,6}	4.5	42.6		SO ₂ /131274.9	
131401.247.....	13 _{10,4} –13 _{9,5}	3.7	39.4	Not observed	(CH ₃) ₂ O/131405.8	(CH ₃) ₂ O/131405.8
131401.247.....	13 _{10,3} –13 _{9,4}	3.7	39.4			
131423.488.....	19 _{3,16} –18 _{3,15}	18.1	42.6	Not observed	Detected	Detected
131491.748.....	12 _{10,2} –12 _{9,3}	2.9	36.5		T_R^* (exp) = 2.7	T_R^* (exp) = 1.5
131491.748.....	12 _{10,3} –12 _{9,4}	2.9	36.5	Not observed	$\sigma = 3.4$	$\sigma = 5.1$
133533.604.....	19 _{6,13} –18 _{6,12}	17.1	47.6	C ₂ H ₃ CN/133534.1	C ₂ H ₃ CN/133534.1	C ₂ H ₃ CN/133534.1
136089.959 ^c	21 _{3,19} –20 _{2,18}	13.6	49.0	CH ₂ CDCN/136091.9 C ₂ H ₃ CN/136094.2 CH ₂ CHOH/136093	CH ₂ CDCN/136091.9 C ₂ H ₃ CN/136094.2 CH ₂ CHOH/136093	CH ₂ CDCN/136091.9 C ₂ H ₃ CN/136094.2 CH ₂ CHOH/136093
136169.967 ^c	22 _{1,21} –21 _{2,20}	17.7	50.3	CH ₃ C ₃ N/136167.2 CH ₃ OD/136171.6 CH ₂ CHOH/136166.4	CH ₃ C ₃ N/136167.2 CH ₃ OD/136171.6 CH ₂ CHOH/136166.4	CH ₃ C ₃ N/136167.2 CH ₃ OD/136171.6 CH ₂ CHOH/136166.4
136174.026 ^c	22 _{2,21} –21 _{2,20}	21.5	50.3	CH ₃ OD/136171.6	CH ₃ OD/136171.6	CH ₃ OD/136171.6
136177.562 ^c	22 _{1,21} –21 _{1,20}	21.5	50.3	<i>c</i> -C ₃ H ₂ /136178.3	<i>c</i> -C ₃ H ₂ /136178.3	<i>c</i> -C ₃ H ₂ /136178.3
136181.621 ^c	22 _{2,21} –21 _{1,20}	17.7	50.3	CH ₃ CH ₂ OH/136180.4	CH ₃ CH ₂ OH/136180.4	CH ₃ CH ₂ OH/136180.4
138777.233.....	37 _{6,31} –37 _{6,32}	1.5	168.6	C ₂ H ₅ CN/138778.7 HCOOCH ₃ /138779.9	C ₂ H ₅ CN/138778.7 HCOOCH ₃ /138779.9	C ₂ H ₅ CN/138778.7 HCOOCH ₃ /138779.9
138877.286.....	20 _{7,14} –19 _{7,13}	17.6	54.9	CH ₂ DCN/138878.3 NH ₂ CN/138879.7	CH ₂ DCN/138878.3 NH ₂ CN/138879.7	CH ₂ DCN/138878.3 NH ₂ CN/138879.7

TABLE 3—Continued

Rest Frequency (MHz) (1)	Transitions (2)	S_{ul} (3)	E_l (cm ⁻¹) (4)	Sgr B2(N-LMH) (5)	Orion KL (6)	W51 e1/e2 (7)
138880.964.....	37 _{6,31} –37 _{5,32}	16.5	168.6	CH ₂ DCN/138878.3 U-133885	CH ₂ DCN/138878.3 U-133885	CH ₂ DCN/138878.3 U-133885
141409.208.....	20 _{6,14} –19 _{6,13}	18.2	52.1	Not observed	SO/141413.1 ^a	SO/141413.1 ^a
141489.981.....	22 _{2,20} –21 _{3,19}	14.7	53.5	Not observed	U-141491 (CH ₃) ₂ CO/141490.5	U-141491; U-141493 (CH ₃) ₂ CO/141490.5
141751.019.....	26 _{11,15} –26 _{10,16}	13.1	103.5	CH ₃ OCHO/141750.3	CH ₃ OCHO/141750.3	CH ₃ OCHO/141750.3
141765.302.....	26 _{11,16} –26 _{10,17}	13.1	103.5	C ₂ H ₅ OH/141768.6 SO ₂ /141757.8	U-141762 SO ₂ /141757.8	C ₂ H ₅ OH/141768.6 U-141762 SO ₂ /141757.8
141782.254.....	22 _{3,20} –21 _{2,19}	14.7	53.5	C ₂ H ₅ OH/141792.0 (CH ₃) ₂ CO/141783.4	C ₂ H ₅ OH/141792.0	C ₂ H ₅ OH/141792.0
142225.352.....	12 _{5,8} –11 _{4,7}	4.6	18.9	Detected	Detected	$T_R^*(\text{exp}) = 1.6$ $\sigma = 2.8$
142300.826.....	21 _{3,18} –20 _{3,17}	20.0	51.5	Detected	HCOOCH ₃ /142293.9	Detected
142323.730.....	25 _{11,14} –25 _{10,15}	12.3	97.5	Not observed	Not observed	HCOOCH ₃ /142326.5 HNO/142328.8
142330.292.....	25 _{11,15} –25 _{10,16}	12.3	97.5	Not observed	Not observed	HCOOCH ₃ /142333.8 NH ₂ CHO/142334.3 HNO/1423330.1
143261.873.....	23 _{11,12} –23 _{10,13}	10.8	86.2	Not observed	U-143263	Not observed
143263.097.....	23 _{11,13} –23 _{10,14}	10.8	86.2			
144839.032 ^c	21 _{9,13} –20 _{9,12}	17.2	66.7	Not observed	<i>c</i> -C ¹³ CCH ₂ /144839.1 DCN/144827.9	<i>c</i> -C ¹³ CCH ₂ /144839.1 DCN/144827.9
144841.834 ^c	21 _{9,12} –20 _{9,11}	17.2	66.7	Not observed	Detected	Detected
144847.127 ^c	21 _{5,17} –20 _{5,16}	19.7	54.1	Not observed	Detected	Detected
144892.195.....	17 _{11,6} –17 _{10,7}	6.2	58.0	Not observed	CH ₂ CDCN/144889.9	CH ₂ CDCN/144889.9
144892.197.....	17 _{11,7} –17 _{10,8}	6.2	58.0		CH ₃ CHO/144896.1 C ₂ H ₅ OH/144893.8	CH ₃ CHO/144896.1 C ₂ H ₅ OH/144893.8
144924.826.....	38 _{6,32} –38 _{6,33}	1.6	177.0	Not observed	¹⁵ NO/144927.8 HC ¹³ CCCCN/144926.8	¹⁵ NO/144927.8 HC ¹³ CCCCN/144926.8
147813.913.....	24 _{1,23} –23 _{1,22}	23.5	59.5	Detected	Not observed	Not observed
147811.758.....	24 _{1,23} –23 _{2,22}	19.7	59.5			
147812.896.....	24 _{2,23} –23 _{2,22}	23.5	59.5			
147814.763.....	22 _{3,19} –21 _{3,18}	20.9	56.3			
147815.051.....	24 _{2,23} –23 _{1,22}	19.7	59.5			
148267.868.....	25 _{0,25} –24 _{0,24}	24.8	60.4	U-148263	Detected	U-148263
148267.851.....	25 _{0,25} –24 _{1,24}	23.6	60.4			
148267.860.....	25 _{1,25} –24 _{1,24}	24.8	60.4			
148267.876.....	25 _{1,25} –24 _{0,24}	23.6	60.4			
149320.892.....	22 _{4,19} –21 _{3,18}	11.3	56.3	CH ₂ CDCN/149320.8 <i>c</i> - ¹³ CCCH ₂ /149320.1 HC ₂ CHO/149322.6 HC ₂ CHO/149318.4	CH ₂ CDCN/149320.8 <i>c</i> - ¹³ CCCH ₂ /149320.1 HC ₂ CHO/149322.6 HC ₂ CHO/149318.4	CH ₂ CDCN/149320.8 <i>c</i> - ¹³ CCCH ₂ /149320.1 HC ₂ CHO/149322.6 HC ₂ CHO/149318.4

TABLE 3—Continued

Rest Frequency (MHz) (1)	Transitions (2)	S_{ul} (3)	E_l (cm ⁻¹) (4)	Sgr B2(N-LMH) (5)	Orion KL (6)	W51 e1/e2 (7)
150909.783.....	22 _{12,11} –21 _{12,10}	15.5	85.9	Detected	$T_R^*(\text{exp}) = 22.9^d$	Detected
150909.784.....	22 _{12,10} –21 _{12,9}	15.5	85.9		$\sigma = 5.5$	
150956.370.....	39 _{6,33} –39 _{5,34}	16.5	185.6	HCOOCH ₃ /150957.2 <i>c</i> -C ₃ H ₂ /150958.1	HCOOCH ₃ /150957.2 <i>c</i> -C ₃ H ₂ /150958.1	HCOOCH ₃ /150957.2 <i>c</i> -C ₃ H ₂ /150958.1
151761.368.....	33 _{3,30} –33 _{2,31}	8.2	123.0	C ₂ H ₅ OH/151756.0	Not observed	Not observed
151764.855.....	33 _{4,30} –33 _{3,31}	8.2	123.0			
151943.485.....	22 _{9,14} –21 _{9,13}	18.3	71.5	Not observed	HCOOCH ₃ /151944.4 C ₂ H ₃ CN/151944.6 HCOOCH ₃ /151950.0 C ₂ H ₃ CN/151936.8	Not observed
151949.778.....	22 _{9,13} –21 _{9,12}	18.3	71.5	Not observed	HCOOCH ₃ /151950.0	Not observed
152048.072.....	37 _{5,32} –37 _{5,33}	1.4	163.6	Not observed	CH ₃ CHO/152048.8 CC ³⁴ S/152050.2	Not observed
152054.930.....	37 _{5,32} –37 _{4,33}	13.7	163.6	Not observed	$T_R^*(\text{exp}) = 1.7$ $\sigma = 21.6$	Not observed
152127.012.....	14 _{5,10} –13 _{4,9}	4.6	24.8	Not observed	C ₂ H ₃ CN/152126.6	Not observed
153632.161.....	25 _{2,24} –24 _{2,23}	24.5	64.5	Not observed	CH ₃ CCH/153629.5	Not observed
153631.563.....	25 _{1,24} –24 _{2,23}	20.7	64.5		CH ₂ (OH)CHO/153633.5	
153632.702.....	25 _{1,24} –24 _{1,23}	24.5	64.5			
153633.299.....	25 _{2,24} –24 _{1,23}	20.7	64.5			
153701.108.....	25 _{5,20} –24 _{6,19}	6.3	77.6	Not observed	CH ₃ OCHO/153700.4	Not observed
154089.088.....	26 _{0,26} –25 _{0,25}	25.8	65.3	<i>c</i> -C ¹³ CCH ₂ /154088.7	<i>c</i> -C ¹³ CCH ₂ /154088.7	<i>c</i> -C ¹³ CCH ₂ /154088.7
154089.080.....	26 _{0,26} –25 _{1,25}	24.6	65.3			
154089.084.....	26 _{1,26} –25 _{1,25}	25.8	65.3			
154089.092.....	26 _{1,26} –25 _{0,25}	24.6	65.3			
154157.076.....	22 _{7,15} –21 _{7,14}	19.8	64.4	<i>c</i> -C ₃ H ₂ /154155.3 CH ₃ CHO/154159.2 CH ¹³ ₃ CH ₂ CN/154145	<i>c</i> -C ₃ H ₂ /154155.3 CH ₃ CHO/154159.2 CH ¹³ ₃ CH ₂ CN/154145	<i>c</i> -C ₃ H ₂ /154155.3 CH ₃ CHO/154159.2 CH ¹³ ₃ CH ₂ CN/154145
156807.010.....	40 _{6,34} –40 _{6,35}	1.6	194.4	Not observed	C ₂ H ₅ CN/156807.8	Not observed
158519.095.....	8 _{8,0} –7 _{7,1}	7.5	17.7	HCOOCH ₃ /158518.0	HCOOCH ₃ /158518.0	HCOOCH ₃ /158518.0
158519.095.....	8 _{8,1} –7 _{7,0}	7.5	17.7			
158554.836.....	23 _{10,14} –22 _{10,13}	18.7	80.9	H ¹³ COOH/158553.4	H ¹³ COOH/158553.4	H ¹³ COOH/158553.4
158555.599.....	23 _{10,13} –22 _{10,12}	18.7	80.9	HC ₂ CHO/158555.6	HC ₂ CHO/158555.6	HC ₂ CHO/158555.6
158629.504.....	19 _{12,7} –19 _{11,8}	7.0	71.3	C ¹³ CS/158625.8	C ¹³ CS/158625.8	C ¹³ CS/158625.8
158629.505.....	19 _{12,8} –19 _{11,9}	7.0	71.3		C ₂ H ₅ CN/158633.5	
158685.793.....	24 _{4,21} –23 _{4,20}	22.9	66.4	C ₂ H ₅ OH/158685.1 H ¹³ CCCN/158692.0	C ₂ H ₅ OH/158685.1	C ₂ H ₅ OH/158685.1 H ¹³ CCCN/158692.0
158688.067.....	16 _{5,12} –15 _{4,11}	4.7	31.7	C ₂ H ₅ OH/158685.1 H ¹³ CCCN/158692.0	C ₂ H ₅ OH/158685.1	C ₂ H ₅ OH/158685.1 H ¹³ CCCN/158692.0
159451.038.....	26 _{1,25} –25 _{2,24}	21.7	69.6	C ₂ H ₃ CN/159449.2	Not observed	C ₂ H ₃ CN/159449.2
159451.351.....	26 _{2,25} –25 _{2,24}	25.5	69.6	SO ₂ /159447.9		SO ₂ /159447.9
159451.636.....	26 _{1,25} –25 _{1,24}	25.5	69.6			
159451.948.....	26 _{2,25} –25 _{1,24}	21.7	69.6			
159791.785.....	23 _{8,16} –22 _{8,15}	20.2	72.8	Not observed	CH ₂ CHCN/159788.2	Not observed

TABLE 3—Continued

Rest Frequency (MHz) (1)	Transitions (2)	S_{ul} (3)	E_l (cm ⁻¹) (4)	Sgr B2(N-LMH) (5)	Orion KL (6)	W51 e1/e2 (7)
159807.072.....	31 _{1,30} –31 _{0,31}	2.8	99.1	HNO/159804.8	HNO/159804.8	Not observed
159807.072.....	31 _{1,30} –31 _{1,31}	0.3	99.1	C ₂ H ₅ OH/159805.9	C ₂ H ₅ OH/159805.9	
159807.084.....	31 _{2,30} –31 _{0,31}	0.3	99.1	C ₂ H ₅ OH/159813.8	C ₂ H ₅ OH/159813.8	
159807.084.....	31 _{2,30} –31 _{1,31}	2.8	99.1	NH ₂ CN/159814.7 CH ₂ DCN/159815.1		
159907.274.....	33 _{8,25} –32 _{9,24}	4.5	140.5	<i>c</i> - ¹³ CCCH/159909.7 CH ₂ CDCN/159907.5	<i>c</i> - ¹³ CCCH/159909.7 CH ₂ CDCN/159907.5	Not observed
159910.073.....	27 _{0,27} –26 _{0,26}	26.8	70.5	<i>c</i> - ¹³ CCCH/159910	<i>c</i> - ¹³ CCCH/159910	Not observed
159910.069.....	27 _{0,27} –26 _{1,26}	25.6	70.5	NH ₂ CN/159919.6	NH ₂ CN/159919.6	
159910.071.....	27 _{1,27} –26 _{1,26}	26.8	70.5	CH ₂ CDCN/159907.4	CH ₂ CDCN/159907.4	
159910.075.....	27 _{1,27} –26 _{0,26}	25.6	70.5			
159963.606.....	23 _{8,15} –22 _{8,14}	20.2	72.8	U-159967	U-159967	Not observed
159965.186.....	22 _{3,17} –21 _{5,16}	21.0	60.0	<i>l</i> - ¹³ CCCH ₂ /159960 (CH ₃) ₂ CO/159964.5	<i>l</i> - ¹³ CCCH ₂ /159960 (CH ₃) ₂ CO/159964.5	Not observed
160153.458.....	23 _{6,18} –22 _{6,17}	21.4	66.6	U-160144	U-160144	Detected
164851.302.....	26 _{2,24} –25 _{3,23}	18.8	73.5	Not observed	Detected	U-164850
164861.611.....	26 _{3,24} –25 _{3,23}	25.2	73.5	Not observed	Detected	Detected
164870.010.....	26 _{2,24} –25 _{2,23}	25.2	73.5	Not observed	Detected	$T_R^*(\text{exp}) = 11.6$ $\sigma = 4.0$
164880.319.....	26 _{3,24} –25 _{2,23}	18.8	73.5	Not observed	Detected	$T_R^*(\text{exp}) = 3.9$ $\sigma = 4.0$
164886.186.....	24 _{12,13} –23 _{12,12}	18.0	96.2	Not observed	Detected	$T_R^*(\text{exp}) = 12.6^c$ $\sigma = 4.0$
164886.189.....	24 _{12,12} –23 _{12,11}	18.0	96.2			
165159.782.....	32 _{1,31} –32 _{0,32}	2.8	105.4	SO ₂ /165144.6	Not observed	Not observed
165159.782.....	32 _{1,31} –32 _{1,32}	0.3	105.4	C ₂ H ₃ CN/165148.3		
165159.788.....	32 _{2,31} –32 _{0,32}	0.3	105.4			
165159.788.....	32 _{2,31} –32 _{1,32}	2.8	105.4			
165211.700.....	24 _{11,14} –23 _{11,13}	19.0	91.0	(CH ₃) ₂ O/165208.9	(CH ₃) ₂ O/165208.9	(CH ₃) ₂ O/165208.9
165211.784.....	24 _{11,13} –23 _{11,12}	19.0	91.0			
165252.331.....	21 _{3,17} –20 _{4,16}	6.8	53.5	U-165254 C ₂ H ₃ CN/165258.6	$T_R^*(\text{exp}) = 3.4$ $\sigma = 4.1$	$T_R^*(\text{exp}) = 1.8$ $\sigma = 3.5$
165270.602.....	27 _{1,26} –26 _{1,25}	26.5	74.9	Detected	$T_R^*(\text{exp}) = 66.2^f$ $\sigma = 6.9$	Detected
165270.289.....	27 _{1,26} –26 _{2,25}	22.7	74.9			
165270.452.....	27 _{2,26} –26 _{2,25}	26.5	74.9			
165270.765.....	27 _{2,26} –26 _{1,25}	22.7	74.9			
165274.262.....	26 _{5,21} –25 _{6,20}	7.5	83.3	HCOOCH ₃ /165258.6	HCOOCH ₃ /165258.6	HCOOCH ₃ /165258.6
165337.372.....	9 _{8,2} –8 _{7,1}	7.4	19.5	U-165340	U-165340	U-165340
165337.372.....	9 _{8,1} –8 _{7,2}	7.4	19.5			
165647.364.....	24 _{10,15} –23 _{10,14}	19.9	86.2			
165649.119.....	24 _{10,14} –23 _{10,13}	19.9	86.2	HCOOCH ₃ /165657.4	HCOOCH ₃ /165657.4	HCOOCH ₃ /165657.4
165730.808.....	28 _{0,28} –27 _{0,27}	27.8	75.8	C ¹³ CS/165729.4	C ¹³ CS/165729.4	C ¹³ CS/165729.4
165730.806.....	28 _{0,28} –27 _{1,27}	26.6	75.8			
165730.808.....	28 _{1,28} –27 _{1,27}	27.8	75.8			
165730.810.....	28 _{1,28} –27 _{0,27}	26.6	75.8			

TABLE 3—Continued

Rest Frequency (MHz) (1)	Transitions (2)	S_{ul} (3)	E_l (cm ⁻¹) (4)	Sgr B2(N-LMH) (5)	Orion KL (6)	W51 e1/e2 (7)
202553.630.....	29 _{9,21} –28 _{9,20}	26.2	112.0	SO ₂ /202562.5 CH ₃ CN/202567.9 C ₂ H ₃ CN/202529.8 HCOOH/202530.0	SO ₂ /202562.5 CH ₃ CN/202567.9 C ₂ H ₃ CN/202529.8 HCOOH/202530.0	SO ₂ /202562.5 CH ₃ CN/202567.9 C ₂ H ₃ CN/202529.8 HCOOH/202530.0
202594.926.....	39 _{1,38} –39 _{0,39}	2.8	155.0	C ₂ HCHOH/202588.3	C ₂ HCHOH/202588.3	C ₂ HCHOH/202588.3
202594.926.....	39 _{2,38} –39 _{1,39}	2.8	155.0			
202594.926.....	39 _{1,38} –39 _{1,39}	0.3	155.0			
202594.926.....	39 _{2,38} –39 _{0,39}	0.3	155.0			
205077.995.....	31 _{4,27} –30 _{4,26}	29.7	111.6	Not observed	CH ₃ CCH/205076.8 (CH ₃) ₂ O/205075.2	CH ₃ CCH/205076.8 (CH ₃) ₂ O/205075.2
205184.844.....	32 _{3,29} –31 _{4,28}	21.8	114.2	Not observed	<i>c</i> - ¹³ CCCH ₂ /205184.2 <i>c</i> -C ₂ H ₄ O/205174.8	<i>c</i> - ¹³ CCCH ₂ /205184.2 <i>c</i> -C ₂ H ₄ O/205174.8
205191.388.....	32 _{4,29} –31 _{4,28}	30.9	114.2	Not observed	C ₂ H ₃ CN/205194.5	C ₂ H ₃ CN/205194.5
205196.595.....	32 _{3,29} –31 _{3,28}	30.9	114.2	Not observed	C ₂ H ₃ CN/205194.5 C ₂ H ₃ CN/205201.9	C ₂ H ₃ CN/205194.5 C ₂ H ₃ CN/205201.9
205203.139.....	32 _{4,29} –31 _{3,28}	21.8	114.2	Not observed	C ₂ H ₃ CN/205201.9	C ₂ H ₃ CN/205201.9
205559.895.....	33 _{3,31} –32 _{3,30}	32.2	116.1	Detected	T_R^* (exp) = 63.7 ^e σ = 9.0	Detected
205559.761.....	33 _{2,31} –32 _{3,30}	25.9	116.1			
205560.014.....	33 _{2,31} –32 _{2,30}	32.2	116.1			
205560.149.....	33 _{3,31} –32 _{2,30}	25.9	116.1			
206369.133.....	30 _{14,17} –29 _{14,16}	23.5	144.6	HCOOCH ₃ /206371.1	HCOOCH ₃ /206371.1	HCOOCH ₃ /206371.1
206369.134.....	30 _{14,16} –29 _{14,15}	23.5	144.6	HCOOD/206372.6	HCOOD/206372.6	HCOOD/206372.6
206440.558.....	13 _{9,5} –12 _{8,4}	8.5	32.6	C ₂ H ₅ CN/206438.2	C ₂ H ₅ CN/206438.2	C ₂ H ₅ CN/206438.2
206440.566.....	13 _{9,4} –12 _{8,5}	8.5	32.6	C ₂ H ₅ CN/206434.3	C ₂ H ₅ CN/206434.3	C ₂ H ₅ CN/206434.3
206468.023.....	35 _{0,35} –34 _{1,34}	33.6	118.6	Detected	Detected	Detected
206468.023.....	35 _{0,35} –34 _{0,34}	34.8	118.6			
206468.023.....	35 _{1,35} –34 _{0,34}	33.6	118.6			
206468.023.....	35 _{1,35} –34 _{1,34}	34.8	118.6			
207938.345.....	40 _{2,39} –40 _{0,40}	0.3	162.8	HCOOCH ₃ /207925.0	HCOOCH ₃ /207925.0	HCOOCH ₃ /207925.0
207938.345.....	40 _{1,39} –40 _{0,40}	2.8	162.8	C ₂ H ₅ C ¹⁵ N/207926.1	C ₂ H ₅ C ¹⁵ N/207926.1	C ₂ H ₅ C ¹⁵ N/207926.1
207938.345.....	40 _{2,39} –40 _{1,40}	2.8	162.8	U-207937	U-207937	U-207937
207938.345.....	40 _{1,39} –40 _{1,40}	0.3	162.8			
207946.288.....	30 _{11,20} –29 _{11,19}	26.0	127.6	C ₂ H ₅ CN/207948.9 <i>c</i> - ¹³ CCCH ₂ /207949.7	C ₂ H ₅ CN/207948.9 <i>c</i> - ¹³ CCCH ₂ /207949.7	C ₂ H ₅ CN/207948.9 <i>c</i> - ¹³ CCCH ₂ /207949.7
207956.271.....	30 _{11,19} –29 _{11,18}	26.0	127.6	C ₂ H ₅ CN/207948.9 <i>c</i> - ¹³ CCCH ₂ /207949.7	C ₂ H ₅ CN/207948.9 <i>c</i> - ¹³ CCCH ₂ /207949.7	C ₂ H ₅ CN/207948.9 <i>c</i> - ¹³ CCCH ₂ /207949.7
208424.845.....	31 _{5,26} –30 _{6,25}	13.9	115.4	Not observed	CH ₂ DCN/208411.6 C ₂ H ₅ CN/208410.9 U-208423	Not observed
208812.515.....	36 _{8,28} –35 _{9,27}	6.4	164.4	Not observed	HCOOCH ₃ /208817.3	Not observed
208841.324.....	30 _{10,21} –29 _{10,20}	26.7	122.9	Not observed	T_R^* (exp) = 18.5 σ = 13.1	Not observed
212286.362.....	36 _{0,36} –35 _{1,35}	34.6	125.5	Detected	NH ₂ CHO/212277.0	NH ₂ CHO/212277.0
212286.362.....	36 _{0,36} –35 _{0,35}	35.8	125.5			
212286.362.....	36 _{1,36} –35 _{0,35}	34.6	125.5			
212286.362.....	36 _{1,36} –35 _{1,35}	35.8	125.5			

TABLE 3—Continued

Rest Frequency (MHz) (1)	Transitions (2)	S_{ul} (3)	E_l (cm ⁻¹) (4)	Sgr B2(N-LMH) (5)	Orion KL (6)	W51 e1/e2 (7)
216766.194.....	19 _{7,13} –18 _{6,12}	6.6	47.7	Not observed	SO ₂ /216758.6 18OCS/216753.5 C ₂ H ₅ CN/216752.5	Not observed
216801.848 ^c	34 _{3,31} –33 _{4,30}	23.9	128.0	Not observed	<i>c</i> -C ₃ H ₂ /216808.7	Not observed
216803.841 ^c	34 _{4,31} –33 _{4,30}	32.9	128.0		HC ₂ CHO/216803.6	
216805.470 ^c	34 _{3,31} –33 _{3,30}	32.9	128.0		HC ₂ CHO/216806.9	
216807.463 ^c	34 _{4,31} –33 _{3,30}	23.9	128.0		HCOOCH ₃ /216808.9 CH ₃ COOH/216811.6 C ₂ H ₅ OH/216813.2	
217080.660.....	32 _{5,27} –31 _{5,26}	30.5	122.4	Not observed	SiO/217104.9 33SO ₂ /217105 SO ¹⁸ O/217102.7	Not observed
217188.885 ^c	35 _{2,33} –34 _{3,32}	27.8	130.0	Not observed	(CH ₃) ₂ O/217189.7	Not observed
217188.922 ^c	35 _{3,33} –34 _{3,32}	34.2	130.0		HCOOCH ₃ /217194.4	
217188.956 ^c	35 _{2,33} –34 _{2,32}	34.2	130.0		C ₂ H ₅ C ¹⁵ N/217193.7	
217188.994 ^c	35 _{3,33} –34 _{2,32}	27.8	130.0		(CH ₃) ₂ O/217193.2	
217252.205 ^c	31 _{8,24} –30 _{8,23}	28.9	122.2	Not observed	DCN/217238.6	Not observed
222296.384.....	34 _{4,30} –33 _{5,29}	20.7	132.7	HCOOCH ₃ /222293.3 C ₂ H ₃ CN/222303.7	Not observed	Not observed
222333.715.....	34 _{5,30} –33 _{5,29}	32.6	132.7	<i>c</i> -C ₃ H ₂ /222333.1 <i>c</i> -C ₃ HD/222332.1 C ₂ H ₃ CN/222321.3	Not observed	Not observed
222361.091.....	34 _{4,30} –33 _{4,29}	32.6	132.7	HCOOCH ₃ /222355.5	Not observed	Not observed
222398.422.....	34 _{5,30} –33 _{4,29}	20.7	132.7	C ₂ H ₅ OH/222404.0 C ₂ H ₃ CN/222406.4 C ₂ H ₅ OH/222419.9 HCOOCH ₃ /222421.4 C ₂ H ₃ CN/222422.4	Not observed	Not observed
223003.339.....	36 _{3,34} –35 _{3,33}	35.2	137.3	Detected	T_R^* (exp) = 60.8 ^h σ = 6.8	Not observed
223003.319.....	36 _{2,34} –35 _{3,33}	28.9	137.3			
223003.357.....	36 _{2,34} –35 _{2,33}	35.2	137.3			
223003.376.....	36 _{3,34} –35 _{2,33}	28.9	137.3			
228419.333.....	36 _{3,33} –35 _{3,32}	34.9	142.7	Detected	Detected	Detected
228418.243.....	36 _{3,33} –35 _{4,32}	25.9	142.7			
228418.836.....	36 _{4,33} –35 _{4,32}	34.9	142.7			
228419.927.....	36 _{4,33} –35 _{3,32}	25.9	142.7			
228766.958.....	34 _{6,29} –33 _{5,28}	17.3	137.0	C ₂ H ₃ CN/228769.6 CH ₃ CHO/228760.5	C ₂ H ₃ CN/228769.6 CH ₃ CHO/228760.5	C ₂ H ₃ CN/228769.6 CH ₃ CHO/228760.5
228817.617.....	37 _{2,35} –36 _{3,34}	29.9	144.7	Not observed	C ₂ H ₅ OH/228818.9	C ₂ H ₅ OH/228818.9
228817.628.....	37 _{3,35} –36 _{3,34}	36.2	144.7		HC ₃ N/228821.7	HC ₃ N/228821.7
228817.637.....	37 _{2,35} –36 _{2,34}	36.2	144.7			
228817.647.....	37 _{3,35} –36 _{2,34}	29.9	144.7			
230348.069.....	33 _{6,27} –32 _{6,26}	31.3	133.1	<i>c</i> -C ₂ H ₄ O/230356.5 CH ₃ OH/230368.7 (CH ₃) ₂ O/230368	Detected	Detected
233909.402.....	36 _{4,32} –35 _{5,31}	22.8	147.8	Not observed	T_R^* (exp) = 5.4 σ = 7.4	Not observed

TABLE 3—Continued

Rest Frequency (MHz) (1)	Transitions (2)	S_{ul} (3)	E_l (cm ⁻¹) (4)	Sgr B2(N-LMH) (5)	Orion KL (6)	W51 e1/e2 (7)
233916.346.....	15 _{10,6} –14 _{9,5}	9.5	42.6	Not observed	C ₂ H ₃ CN/233913.6	Not observed
233916.348.....	15 _{10,5} –14 _{9,6}	9.5	42.6		<i>c</i> -C ₃ H ₂ /233914.2 C ₂ H ₅ C ¹⁵ N/233915.2	
233921.548.....	36 _{5,32} –35 _{5,31}	34.6	147.8	Not observed	HO ¹³ CO ⁺ /233921.1 C ₂ H ₅ C ¹⁵ N/233915.2	Not observed
233930.772.....	36 _{4,32} –35 _{4,31}	34.6	147.8	Not observed	CH ₃ OCHO/233926.4	Not observed
233942.919.....	36 _{5,32} –35 _{4,31}	22.8	147.8	Not observed	C ₂ H ₅ OH/233951.1	Not observed
233961.602.....	35 _{5,30} –34 _{5,29}	33.4	144.7	Not observed	HOCO ⁺ /233958.3 CH ₂ CDCN/233967.2 SO ¹⁸ O/233967.4	Not observed
235528.673.....	34 _{6,28} –33 _{6,27}	32.3	140.8	SO ¹⁸ O/235521.0 C ₂ H ₅ OH/235523.9 HCC ¹³ CN/235532.3 C ₂ HCHOH/235532.1	Not observed	HCC ¹³ CN/235532.3 C ₂ HCHOH/235532.1
235556.152.....	40 _{0,40} –39 _{0,39}	39.8	155.0	C ₂ H ₃ CN/235563	Not observed	C ₂ H ₃ CN/235563
235556.152.....	40 _{0,40} –39 _{1,39}	38.6	155.0			CH ₃ CHO/235553.1
235556.152.....	40 _{1,40} –39 _{0,39}	38.6	155.0			
235556.152.....	40 _{1,40} –39 _{1,39}	39.8	155.0			
240035.798.....	38 _{3,35} –37 _{3,34}	36.9	158.1	Not observed	HCOOCH ₃ /240034.6	Not observed
240035.477.....	38 _{3,35} –37 _{4,34}	27.9	158.1			
240035.650.....	38 _{4,35} –37 _{4,34}	36.9	158.1			
240035.972.....	38 _{4,35} –37 _{3,34}	27.9	158.1			
240122.641.....	33 _{8,25} –32 _{8,24}	31.3	137.9	Not observed	CH ₃ C ₄ H/240126.2 NH ₂ CN/240132.7	Not observed
240211.992.....	18 _{9,10} –17 _{8,9}	8.7	49.7	Not observed	T_R^* (exp) = 6.4 σ = 9.5	Not observed
240215.068.....	18 _{9,9} –17 _{8,10}	8.7	49.7	Not observed	T_R^* (exp) = 6.4 σ = 9.5	Not observed
240810.892.....	35 _{6,29} –34 _{6,28}	33.2	148.6	³³ SO ₂ /240810.7	³³ SO ₂ /240810.7	³³ SO ₂ /240810.7 NH ₂ CN/240817.4
240899.571.....	40 _{1,39} –39 _{2,38}	35.8	161.7	Detected	Detected	Detected
240899.571.....	40 _{1,39} –39 _{1,38}	39.5	161.7			
240899.571.....	40 _{2,39} –39 _{1,38}	35.8	161.7			
240899.571.....	40 _{2,39} –39 _{2,38}	39.5	161.7			
240987.760.....	14 _{11,3} –13 _{10,4}	10.4	43.8	H ₂ CCHCN/240987.6	H ₂ CCHCN/240987.6	H ₂ CCHCN/240987.6
240987.760.....	14 _{11,4} –13 _{10,3}	10.4	43.8	(CH ₃) ₂ O/240985.2 C ₂ H ₃ CN/240986.8	(CH ₃) ₂ O/240985.2 C ₂ H ₃ CN/240986.8	(CH ₃) ₂ O/240985.2 C ₂ H ₃ CN/240986.8
241372.658.....	41 _{1,41} –40 _{0,40}	39.6	162.8	C ₂ H ₅ OH/241381.8	T_R^* (exp) = 61.6 ⁱ σ = 5.9	Detected
241372.658.....	41 _{0,41} –40 _{0,40}	40.8	162.8	U-241367		
241372.658.....	41 _{1,41} –40 _{1,40}	40.8	162.8	HCOOCH ₃ /241363.5		
241372.658.....	41 _{0,41} –40 _{1,40}	39.6	162.8			
243791.882.....	35 _{8,28} –34 _{8,27}	33.0	152.5	<i>c</i> -C ₂ H ₄ O/243790.4 CH ₂ CDCN/243787.4 (CH ₃) ₂ O/243797.7	<i>c</i> -C ₂ H ₄ O/243790.4 CH ₂ CDCN/243787.4 (CH ₃) ₂ O/243797.7	<i>c</i> -C ₂ H ₄ O/243790.4 CH ₂ CDCN/243787.4 (CH ₃) ₂ O/243797.7

TABLE 3—Continued

Rest Frequency (MHz) (1)	Transitions (2)	S_{ul} (3)	E_l (cm ⁻¹) (4)	Sgr B2(N-LMH) (5)	Orion KL (6)	W51 e1/e2 (7)
245155.493.....	21 _{8,14} –20 _{7,13}	7.7	59.5	CH ₂ ND/245157 C ₂ H ₅ OH/245159.1 HCOOCH ₃ /245165.8 CH ₃ CHO/245166.4 ³⁴ SO ₂ /245178.7	CH ₂ ND/245157 HCOOCH ₃ /245165.8 CH ₃ CHO/245166.4 ³⁴ SO ₂ /245178.7	CH ₂ ND/245157 HCOOCH ₃ /245165.8 CH ₃ CHO/245166.4 ³⁴ SO ₂ /245178.7
245202.622.....	36 _{7,30} –35 _{7,29}	34.2	156.8	C ₂ H ₅ OH/245202.1 HDCO/245203.1	C ₂ H ₅ OH/245202.1 HDCO/245203.1	C ₂ H ₅ OH/245202.1 HDCO/245203.1
245336.941.....	37 _{6,32} –36 _{6,31}	35.4	160.5	SO ₂ /245339.2 HC ₂ CHO/245339.4	SO ₂ /245339.2 HC ₂ CHO/245339.4	SO ₂ /245339.2 HC ₂ CHO/245339.4
245797.806.....	21 _{8,13} –20 _{7,14}	7.7	59.5	C ₂ H ₃ CN/245808.8 <i>c</i> -C ₃ H ₂ /245797.5 C ₂ H ₅ OH/245803.9	Not observed	C ₂ H ₃ CN/245808.8 <i>c</i> -C ₃ H ₂ /245797.5 C ₂ H ₅ OH/245803.9
245838.545.....	35 _{9,27} –34 _{9,26}	32.7	156.2	$T_R^*(\text{exp}) = 13.0$ $\sigma = 11.4$	Not observed	$T_R^*(\text{exp}) = 7.9$ $\sigma = 9.2$
245844.567.....	39 _{3,36} –38 _{3,35}	37.9	166.1	U-245848	Not observed	U-245848
245844.487.....	39 _{4,36} –38 _{4,35}	37.9	166.1			
245844.660.....	39 _{4,36} –38 _{3,35}	29.0	166.1			
245844.394.....	39 _{3,36} –38 _{4,35}	29.0	166.1			
251220.408.....	38 _{6,33} –37 _{5,32}	21.7	168.6	SO ¹⁸ O/251218.7 C ₂ H ₅ CN/251217.6 C ₂ H ₅ OH/251216.0 SO ₂ /251199.7	Not observed	SO ¹⁸ O/251218.7 C ₂ H ₅ CN/251217.6 C ₂ H ₅ OH/251216.0 SO ₂ /251199.7
251311.985.....	39 _{5,35} –38 _{5,34}	37.6	171.8	C ₂ H ₃ CN/251312.6	Not observed	C ₂ H ₃ CN/251312.6
251309.837.....	39 _{4,35} –38 _{5,34}	25.9	171.8	C ₂ H ₅ C ¹⁵ N/251311.0		C ₂ H ₅ C ¹⁵ N/251311.0
251313.686.....	39 _{4,35} –38 _{4,34}	37.6	171.8	N ₂ O/251311.3		N ₂ O/251311.3
251315.833.....	39 _{5,35} –38 _{4,34}	25.9	171.8	<i>c</i> -C ₃ H ₂ /251314.3		<i>c</i> -C ₃ H ₂ /251314.3

^a At the band edge.

^b Located at bad filter-bank channels.

^c Transitions also observed by Combes et al. 1996 toward Orion KL.

^d Improper pointing solution applied plus high humidity.

^e The actual observed T_R^* is at 7.2 mK, which is below 3 σ . If the uncertainty of the rotation diagram fit is considered, the minimum expected T_R^* is at 4.8 mK.

^f Tuning error plus off-scale amplitude gain.

^g Two-thirds of data suffered from high T_{sys} and high wind; another one-third were taken when the mixers were behaving abnormally.

^h Large gain variation in one mixer plus problem with pointing and focus.

ⁱ Problem with pointing and focus.

we found that, after carefully inspecting all spectra gathered, the glycine spectral features identified in Sgr B2 tend to be slightly redshifted toward higher velocities, while those in Orion and W51 tend to be blueshifted in an opposite sense with respect to the nominal velocities. A number of well-defined spectral features close to presumed glycine frequencies, as well as being simultaneously detected in Sgr B2 and in either Orion or W51, were discarded because they shifted the wrong way, i.e., moving in the same sense in velocity. It was concluded that spectral features exhibiting such behavior were from transitions of other unknown or known molecular species, at frequencies slightly higher or lower than the glycine transitions sought. For instance, glycine “look-alike” spectral features at $V_{\text{LSR}} \gtrsim 70 \text{ km s}^{-1}$ in Sgr B2 were abandoned subject to this criterion.

To further illustrate this, consider Figures 2*a* and 2*b*. The spectral feature immediately to the left of the identified glycine line in W51 (U-165268) can be immediately ruled out;

otherwise, we could be easily confused by the two adjacent spectral features, with the left one being erroneously assigned a V_{LSR} of 64.5 km s⁻¹. Although such potential misidentifications are less likely in spectra of W51 e1/e2, they could be very misleading in those of Sgr B2(N-LMH), where a “reasonable” V_{LSR} can be anywhere between 58 and 75 km s⁻¹. Neglecting the possible effects of partial line-blendings and uncertainties in frequency, due to the spectral resolution employed and adopted rest frequencies, we find that the LSR velocities of glycine emission are in the ranges ~63–68, ~5–8, and ~56–60 km s⁻¹ in Sgr B2(N-LMH), Orion KL, and W51 e1/e2, respectively (Table 2).

The observation that the glycine lines in Orion KL cover a V_{LSR} range from ~5 km s⁻¹ (the “hot core” velocity) to ~8 km s⁻¹ (the “compact ridge” velocity) implies that the glycine emission within our 12 m beams may come from both the hot core and compact ridge. As clearly indicated by Wright, Plambeck, & Wilner (1996), however, the many

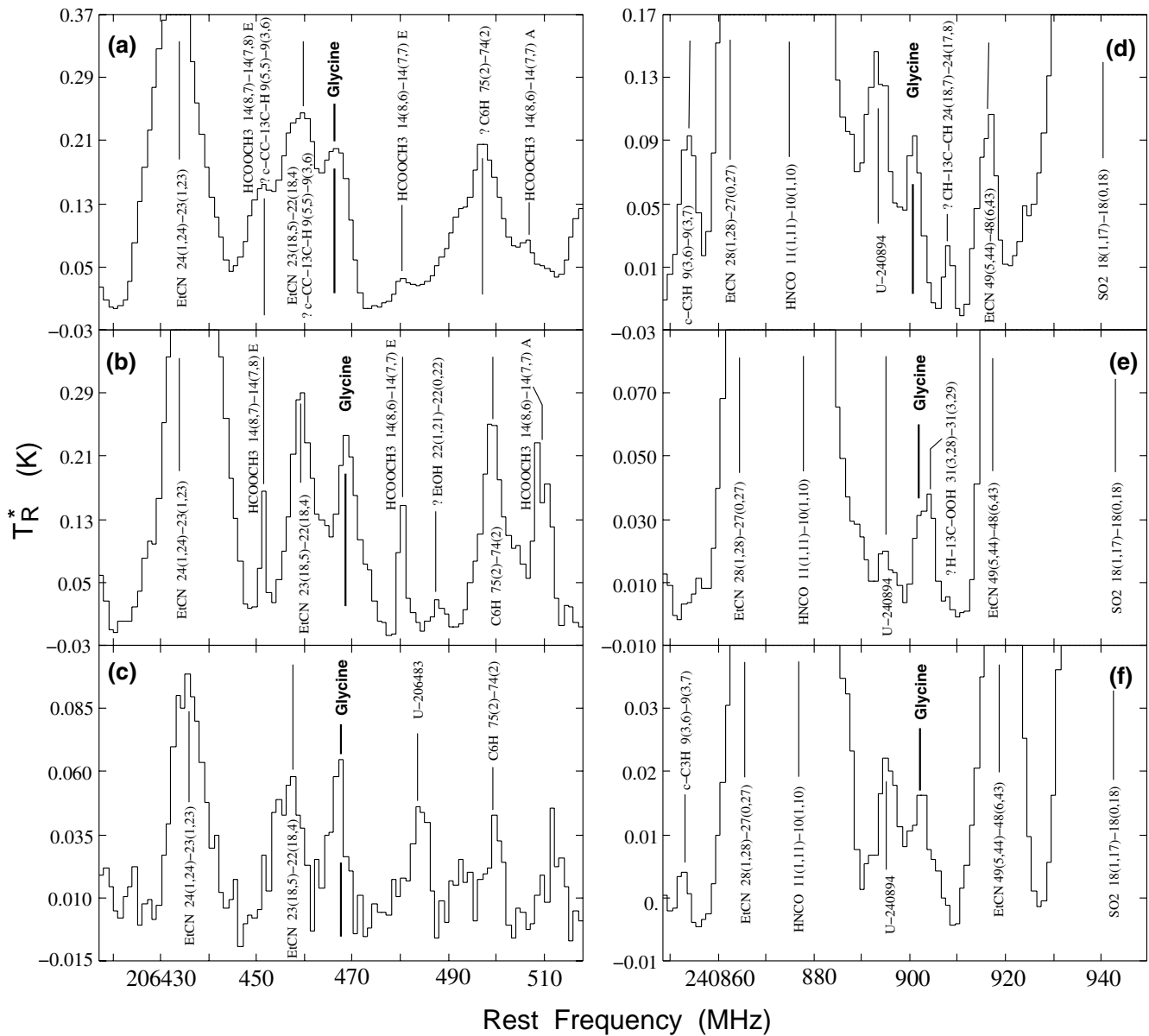


FIG. 1.—Glycine spectra (at 1 MHz resolution) observed at 206,468 MHz (line 21) in (a) Sgr B2(N-LMH), (b) Orion KL, and (c) W51 e1/e2 and at 240,899 MHz (line 26) in (d) Sgr B2(N-LMH), (e) Orion KL, and (f) W51 e1/e2. The abscissae give the rest frequencies based on the assumed LSR velocities: 64.0, 8.0, and 60.0 km s⁻¹ for Sgr B2(N-LMH), Orion KL, and W51 e1/e2, respectively. The thick vertical lines mark the glycine lines at the frequencies corresponding to the velocities listed in Table 2. The thin vertical lines denote the spectral features of other molecular species; question marks indicate uncertain identifications because of overly strong line intensities or inconsistent LSR velocities. The rms noise of each spectrum is listed in Table 2.

spatial substructures and kinematic subcomponents in Orion KL make the velocity fields in Orion fairly complicated. Certain molecules, such as CH₃CN, CH₃OH, and H¹³CN, do not appear to exhibit a clear distinction, either kinematically or spatially, between the compact ridge and hot core (Wright et al. 1996). In their line survey, Lee et al. (2001) found that the location of about half of the molecular species they detected could not be distinguished between the two Orion KL subregions, based on kinematics alone. In addition, among the many single-dish line surveys toward Orion KL to date, there are only a few band scans, such as Blake et al. (1987), Sutton et al. (1995), and Ikeda et al. (2001), that really separate the hot-core and compact-ridge components. Nevertheless, the surveys by Sutton et al. (1995) and Ikeda et al. (2001) are in fact multifield surveys; in other words, the distinction is based on spatial informa-

tion instead of kinematic information. It is interesting to note that in the multifield Orion band scan of Sutton et al. (1995), ~50% of the molecular species observed toward the compact ridge show velocities between 4.4 and 6.4 km s⁻¹; the remaining 50% are at velocities between 6.7 and 9.3 km s⁻¹. Therefore, based only on the measured velocities, no definite conclusion can be drawn here on the precise location of glycine emission in Orion KL (see § 3.3). Accordingly, the average velocities of glycine emission are thus 65.5 ± 1.5 km s⁻¹ toward Sgr B2, 7.0 ± 1.3 km s⁻¹ in Orion, and 58.8 ± 1.4 km s⁻¹ in W51.

3.3. Column Densities

We use the “rotational diagram” method (Cummins, Linke, & Thaddeus 1986; Turner 1991) to derive the column

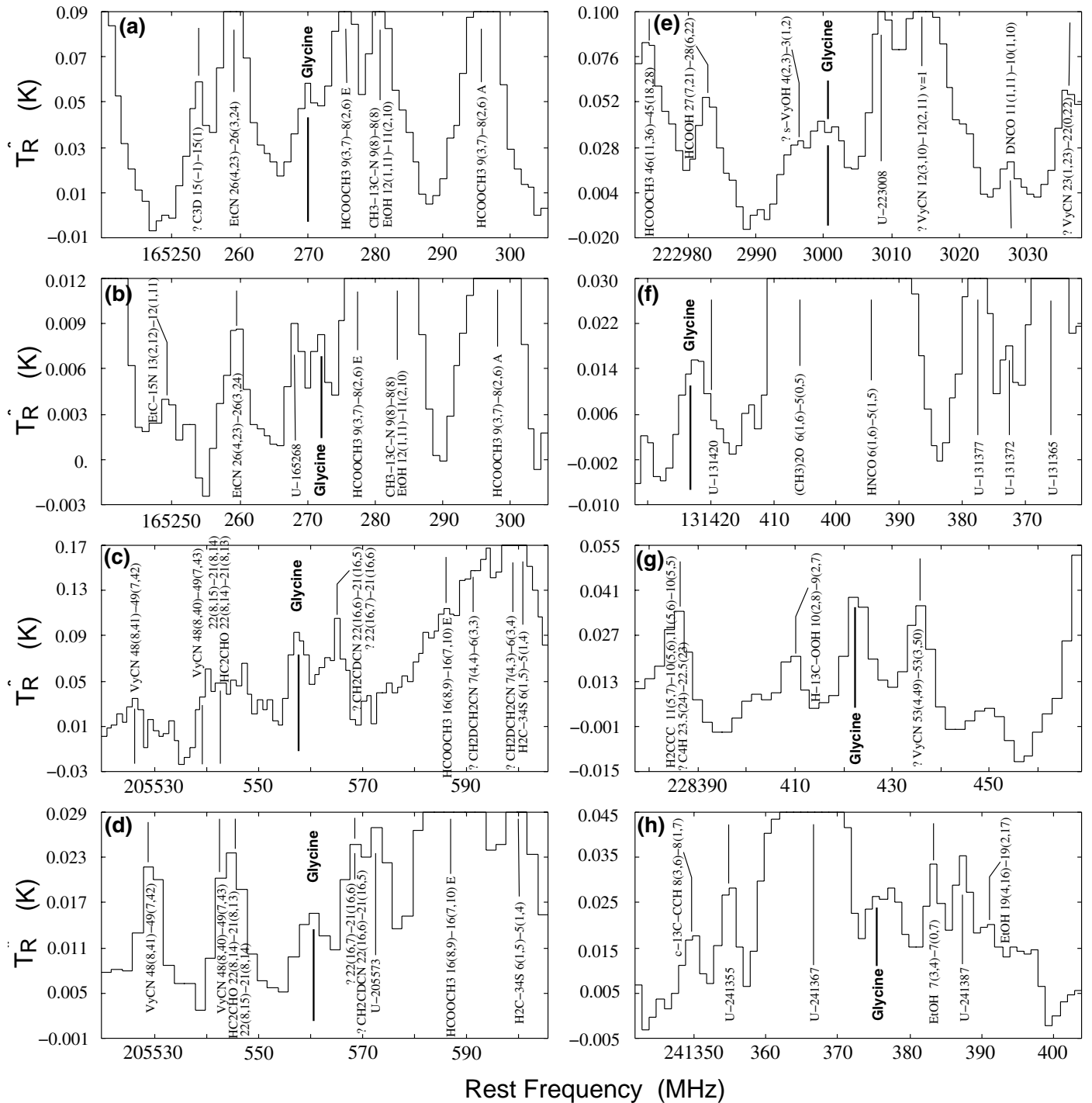


FIG. 2.—Glycine spectra observed at 165,270 MHz (line 19) in (a) Sgr B2(N-LMH) and (b) W51 e1/e2 and at 205,560 MHz (line 20) in (c) Sgr B2(N-LMH) and (d) W51 e1/e2, and also at (e) 223,003 MHz (line 23) in Sgr B2(N-LMH), at (f) 131,423 MHz (line 5) and (g) 228,419 MHz (line 24) in Orion KL, and at (h) 241,372 MHz (line 27) in W51 e1/e2. The spectra illustrated are at 1 MHz resolution, except for the spectra in (d) and (g), which are at 2 MHz resolution. The same figure labels and symbol conventions used in Fig. 1 are adopted here.

densities of glycine. Assuming that the glycine lines are optically thin in LTE and that the rotational excitation temperature, T_{rot} , is much higher than the background brightness temperature, we have

$$\log\left(\frac{3kW_K}{8\pi^3\nu S_{ul}\mu^2}\right) = \log\left(\frac{N_{\text{tot}}}{Q_{\text{rot}}}\right) - \frac{E_u \log(e)}{kT_{\text{rot}}}, \quad (1)$$

where $W_K = \int T_R^* dv$ is the integrated intensity, ν is the rest

frequency, μ the permanent dipole moment, S_{ul} the line strength, E_u the upper energy level, Q_{rot} the rotational partition function, and N_{tot} the beam-averaged total column density. For glycine lines that contain more than one glycine transition, a summation of $S_{ul}\mu^2$ over all relevant transitions was used. The rotation diagrams, with linear least-squares fits applied, are shown in Figure 4. Partially blended glycine lines are also included in the fits. For these partially blended lines, line width uncertainties are dominated by line

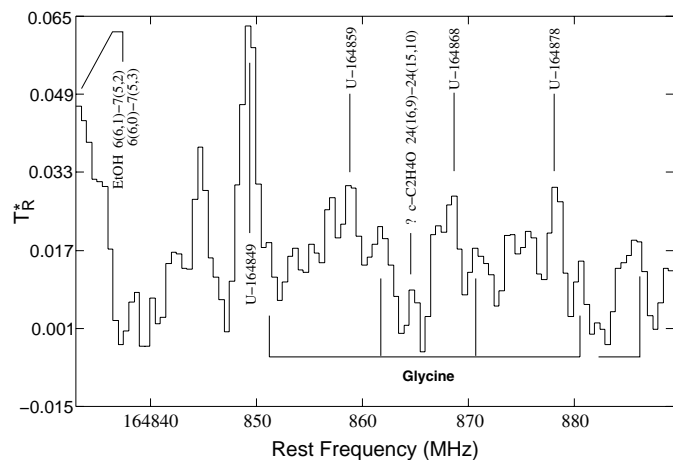


FIG. 3.—Glycine spectrum in Orion (at 500 kHz resolution) of the quadruplet lines at 164.8 GHz (lines 14, 15, 16, and 17), plus the line at 164.886 MHz (line 18). The same figure labels and symbol conventions used in Fig. 1 are adopted here. The expected relative line intensities of the glycine quadruplet and the nearby glycine line, based on the actual fit of the Orion rotation diagram and the measured line widths, are indicated by the thick vertical lines.

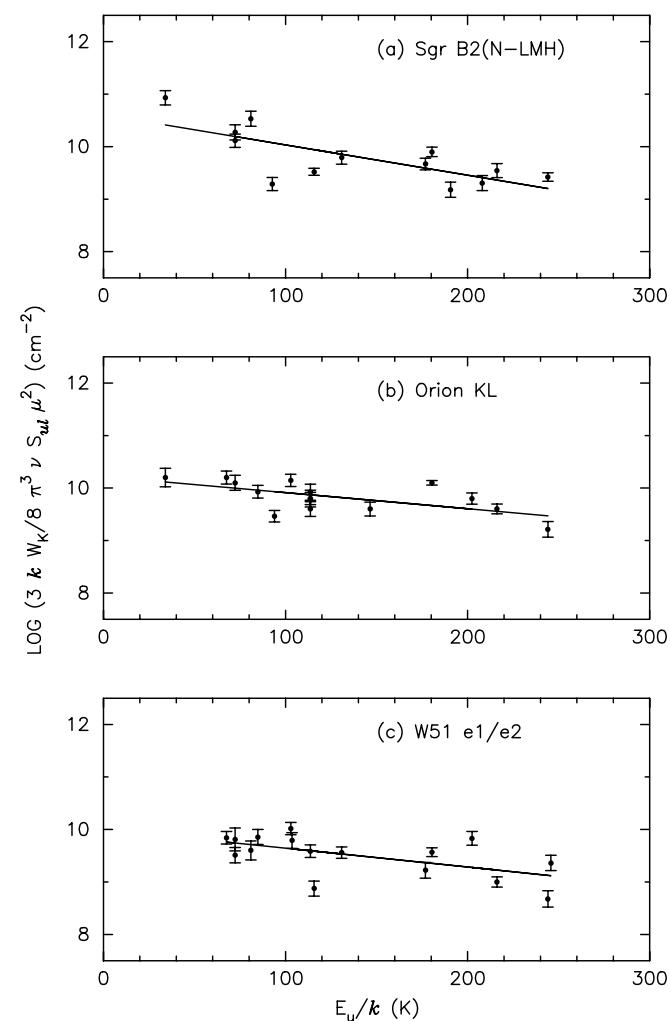


FIG. 4.—Rotation diagrams with linear least-squares fits of the observed glycine lines in (a) Sgr B2(N-LMH), (b) Orion KL, and (c) W51 e1/e2. The error bar is 1σ .

blending (§ 3.1). However, extreme cases of estimation errors of a factor of 2 in line width yield only uncertainties of 0.3 in the logarithmic values of the rotation diagram ordinate. The rather tight fits with small scattering ($\chi^2 = 1.55$ for Sgr B2, 0.74 for Orion, and 1.47 for W51) clearly indicate that the glycine emission is in LTE with a single excitation temperature and is likely from a mostly homogeneous source. Furthermore, the well-delineated fits of the rotation diagrams clearly provide strong evidence that the spectral lines identified are indeed from glycine emission. Sgr B2 appears to have the largest scatter among the three sources; this could be due to partial line-blending of the glycine lines being more prevalent in Sgr B2.

The rotational excitation temperatures thus derived are $T_{\text{rot}} = 75_{-16}^{+29}$, 141_{-37}^{+76} , and 121_{-32}^{+71} K for Sgr B2(N-LMH), Orion KL, and W51 e1/e2, respectively. The derived rotation temperatures of the three HMCs show good agreement with each other, with Orion the hottest and Sgr B2 the lowest, consistent with the general trend in other single-dish observations of large molecules within the uncertainties (Blake et al. 1987; Ohishi et al. 1995; Nummelin et al. 2000; Ikeda et al. 2001). A T_{rot} of 141 K in Orion KL suggests that glycine emission may come mainly from the Orion compact ridge (Blake et al. 1987). The column densities obtained are $N_{\text{tot}} = 4.16_{-1.82}^{+3.22} \times 10^{14}$, $4.37_{-1.27}^{+1.79} \times 10^{14}$, and $2.09_{-0.77}^{+1.22} \times 10^{14} \text{ cm}^{-2}$ for Sgr B2(N-LMH), Orion KL, and W51 e1/e2, respectively. These column densities are essentially the same: within a factor of 2.5 of each other, with Orion being the highest. The column density of Orion KL thus derived is about a factor of 8 higher than the upper limit obtained by Combes et al. (1996). However, if glycine emission is extended as evidently reflected by the tight fit of the rotation diagram of Orion, and in addition is not perfectly centered at the nominal compact-ridge position, then the much smaller IRAM 30 m beams ($13''$ at 1.3 mm and $19''$ at 2 mm) compared to our $45''$ beam at 2 mm and $30''$ beam at 1.3 mm) might have missed a significant portion of the glycine emission. As clearly revealed by interferometer observations, the emission from molecular species such as HCOOH, CH_3CN , CH_3OH , and HCOOCH_3 is not well centered at the compact-ridge position and also is quite extended (e.g., Blake et al. 1996; Wright et al. 1996; Liu et al. 2002). Furthermore, Combes et al. (1996) took their *best* rms noise level at 3 mm to compute the Orion upper limit. This probably means it is a 1σ upper limit. A 3σ upper limit will then be 3 times higher than the reported value of Combes et al. (1996), which makes our number only about a factor of 3 higher. Moreover, Combes et al. (1996) adopted an excitation temperature of 50 K for their calculations; this is a factor of ~ 3 lower than our measured temperature. Because of the partition function, lower excitation temperature usually results in a lower column density.

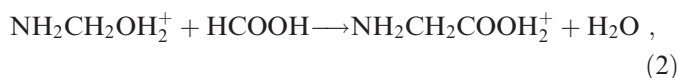
The fractional abundance of glycine with respect to molecular hydrogen, $X_{\text{NH}_2\text{CH}_2\text{COOH}} = N_{\text{NH}_2\text{CH}_2\text{COOH}}/N_{\text{H}_2}$, may also be deduced. H_2 column densities inferred from single-dish observations with beam sizes similar to the 12 m are employed, in order to determine the beam-averaged abundances more accurately. The hydrogen column densities adopted are $\simeq 2 \times 10^{24} \text{ cm}^{-2}$ for Sgr B2(N-LMH) (Nummelin et al. 2000), $3 \times 10^{23} \text{ cm}^{-2}$ for Orion KL (Blake et al. 1987), and $1 \times 10^{24} \text{ cm}^{-2}$ for W51 e1/e2 (Jaffe, Becklin, & Hildebrand 1984). Glycine fractional abundances thus estimated are 2.1×10^{-10} for Sgr B2, 1.5×10^{-9} for Orion, and 2.1×10^{-10} for W51.

4. DISCUSSION: GLYCINE FORMATION

Interstellar glycine molecules reside in warm, dense gas where icy grain mantles have been removed. Thus, they may have been formed on grain surfaces and have been evaporated or synthesized in the gas through reactions among other evaporated molecules (e.g., Charnley, Tielens, & Millar 1992). Here we briefly discuss possible formation mechanisms for interstellar glycine.

Amino acids are very susceptible to destruction by UV photolysis (Ehrenfreund et al. 2001a), but these hot-core amino acids can survive in the gas since the visual extinction in HMCs is large ($A_V \gtrsim 300$). Thus, any energetic UV processing of grain mantles must have occurred in cold molecular cloud material, prior to hot-core formation. Recent experiments (Bernstein et al. 2002; Muñoz-Caro et al. 2002) have shown that UV photolysis of interstellar ice analogs can produce small abundances of glycine and other amino acids. It is not clear if these experiments are able to quantitatively, and in some cases qualitatively, reproduce the distribution of organic molecules observed in hot cores. Sorrell (2001) has suggested that glycine could be formed in UV-photolyzed ice mantles from CH_3COOH in a radical-molecule reaction, by replacing a methyl group hydrogen with an amino group. However, the low expected efficiency of UV photolysis in dark clouds (e.g., Gibb et al. 2000) and the fact that amino acids are photochemically labile (Ehrenfreund et al. 2001a) both raise serious problems for production of amino acids and other complex organics by UV photolysis of interstellar molecular ices.

Alkyl cation transfer reactions (Karpas & Mautner 1989) can produce large organic molecules in gas whose composition is dominated by alcohol molecules (mainly methanol and ethanol) recently evaporated from the dust (Charnley et al. 1995; Charnley, Ehrenfreund, & Kuan 2001). Grain surface chemistry theories that can account for the presence of these alcohols also predict the existence of aminoalcohols ($\text{NH}_2\text{C}_n\text{H}_{2n}\text{OH}$, $n = 1, 2, \dots$) in grain mantles (Charnley 1997). Analogous ion-molecule reactions between protonated aminoalcohols and formic acid, a known and abundant mantle molecule (Ehrenfreund & Schutte 2000; Liu, Mehringer, & Snyder 2001), could produce glycine in the exothermic process (Charnley 1997)



followed by an electron dissociative recombination. Amino-methanol is highly unstable in the laboratory; however, related ion-molecule experiments, involving protonated aminoethanol and HCOOH, appear to suggest that amino-alkyl cation transfer reactions may indeed be a viable pathway for interstellar amino acid synthesis (D. K. Bohme 2002, private communication). Alternatively, some models of dense-cloud gas-grain chemistry predict that hydroxylamine (NH_2OH) could be abundant in interstellar ices (Charnley, Rodgers, & Ehrenfreund 2001). Experiments demonstrate that, in hot cores, evaporated hydroxylamine, once protonated, could react with acetic acid to produce protonated glycine (Blagojevic, Petrie, & Bohme 2003):



Thus, there are two plausible gas-phase pathways to interstellar glycine. Single-dish observations of HCOOH yield column densities of $(0.5\text{--}1.5) \times 10^{14} \text{ cm}^{-2}$ in Orion (Sutton et al. 1985; Blake et al. 1987; Turner 1991) and $(4.2\text{--}11) \times 10^{14} \text{ cm}^{-2}$ in Sgr B2(N-LMH) (Turner 1991; Nummelin et al. 2000). If one assumes a rate coefficient of $\sim 10^{-11} \text{ cm}^3 \text{ s}^{-1}$ for cation transfer processes such as reaction (2), then standard hot-core calculations indicate that a “daughter/parent” abundance ratio (i.e., $\text{NH}_2\text{CH}_2\text{COOH}/\text{HCOOH}$) should be about 0.1, when the “daughter” abundance peaks in the postevaporation gas (Charnley et al. 1995). These observations imply column density ratios of $N_{\text{NH}_2\text{CH}_2\text{COOH}}/N_{\text{HCOOH}} > 1$ and so present severe difficulties for glycine being produced from HCOOH. Interferometric observations will give higher column densities in both sources if the HCOOH emission is spatially compact. Liu et al. (2001) measured N_{HCOOH} equal to $11.0 \times 10^{15} \text{ cm}^{-2}$ in Sgr B2(N-LMH) and $1.9 \times 10^{15} \text{ cm}^{-2}$ in Orion. This gives $N_{\text{NH}_2\text{CH}_2\text{COOH}}/N_{\text{HCOOH}} \sim 0.04$ in Sgr B2(N-LMH) and ~ 0.23 in Orion: closer to what one might expect from ion-molecule chemistry. However, one must be very careful in comparing data from interferometers and single-dish telescopes. For emission from compact sources, array observations will lead to a higher column density than corresponding beam-averaged single-dish observations of the same source. Thus, irrespective of whether glycine emission is compact or not, standard hot-core gas-grain chemistry would appear to have problems explaining its column density relative to HCOOH. This may not simply be an issue of the spatial scale of the glycine emission. BIMA array data, which are compact-component sensitive, indicate that the emission of CH_3COOH and HCOOH in both Sgr B2 (N-LMH) and W51 e1/e2 is not extended. The observed $\text{CH}_3\text{COOH}/\text{HCOOH}$ column density ratios are $\sim 0.6\text{--}1$ (Remijan et al. 2002), and these also present difficulties for theories where CH_3COOH is produced from reactions of protonated methanol with HCOOH (Charnley 1997). The resolution to these discrepancies may lie in the ion-molecule chemistries of the different molecules. It has already been noted that, to account for the large difference between ice- and gas-phase abundances, previously unconsidered processes must act to selectively destroy HCOOH in hot cores (Ehrenfreund et al. 2001b). Since proton transfer from protonated large organic molecules to HCOOH (e.g., alcohols and aminoalcohols) is endothermic, it may be that much of the evaporated HCOOH is converted into organic acids in the gas. High abundance ratios relative to HCOOH would obtain if these compounds, once formed, were destroyed more slowly than formic acid; laboratory studies of the relevant ion-molecule and electron-ion processes could ultimately test this explanation.

To summarize, both ion-molecule chemistry and solid state reactions could conceivably generate a large and diverse group of amino acids, many of which have been identified within the amino acid inventory of the Murchison meteorite (Charnley 2001; Muñoz-Caro et al. 2002). In both cases, more studies are needed to quantify the efficiency of either scenario. Even if it should transpire that interstellar glycine is unconnected to the organic chemistry of protosolar nebula material, and hence to meteoritic composition (e.g., Botta et al. 2002), it nevertheless appears that a population of interstellar amino acids may exist.

5. CONCLUSIONS

In conclusion, 27 glycine lines were detected in 19 different millimeter-wave bands in one or more of the hot molecular cores Sgr B2(N-LMH), Orion KL, and W51 e1/e2. Our analysis of the abundances of $\text{NH}_2\text{CH}_2\text{COOH}$, HCOOH , and CH_3COOH indicates that there is no significant difference between these two potential precursors and glycine; the primary chemical production paths of glycine remain to be determined. This is the first detection of an amino acid in interstellar space and greatly strengthens the thesis that interstellar organic molecules could have played a pivotal role in the prebiotic chemistry of the early Earth. However, the crucial “link” that connects amino acids in space to prebiotic chemistry in the solar system, and perhaps to the emergence of life elsewhere in the Galaxy, is still missing. The discovery of interstellar glycine is only a first step toward answering this question.

We would like to thank Kentarou Kawaguchi for checking against his unpublished spectral line lists and Thomas L. Wilson for his invaluable comments. We are indebted to an anonymous referee for his helpful suggestions and comments that improved the paper. The authors are grateful to the JPL Molecular Spectroscopy Web service (<http://spec.jpl.nasa.gov>) and the Cologne Database for Molecular Spectroscopy Web service (<http://www.ph1.uni-koeln.de/vorhersagen>) for making molecular laboratory data available. We wish to thank the ARO staff and J. P. Schaefer of Research Corporation for continued support of the Kitt Peak 12 m telescope, which enabled the completion of this project. The research of Y.-J. K. was supported by grants NSC 90-2112-M-003-012 and NSC 91-2112-M-003-016. This work was supported by NASA's Exobiology Program through funds allocated by NASA Ames under interchange NCC2-1162 to the SETI Institute.

REFERENCES

- Bernstein, M. P., Dworkin, J. P., Sandford, S. A., Cooper, G. W., & Allamandola, L. J. 2002, *Nature*, 416, 401
- Berulis, I. I., Winnenwiser, G., Krasnov, V. V., & Sorochenko, R. L. 1985, *Soviet Astron. Lett.*, 11, 251
- Blagojevic, V., Petrie, S., & Bohme, D. K. 2003, *MNRAS*, 339, L7
- Blake, G. A., Mundy, L. G., Carlstrom, J. E., Padin, S., Scott, S. L., Scoville, N. Z., & Woody, D. P. 1996, *ApJ*, 472, L49
- Blake, G. A., Sutton, E. C., Masson, C. R., & Phillips, T. G. 1987, *ApJ*, 315, 621
- Botta, O., Glavin, D. P., Kminek, G., & Bada, J. L. 2002, *Origins Life Evol. Biosphere*, 32, 143
- Brown, R. D., Godfrey, P. D., Storey, J. W. V., & Bassez, M.-P. 1978, *J. Chem. Soc. Chem. Commun.*, 547
- Brown, R. D., et al. 1979, *MNRAS*, 186, 5P
- Ceccarelli, C., Loinard, L., Castets, A., Faure, A., & Lefloch, B. 2000, *A&A*, 362, 1122
- Charnley, S. B. 1997, in *IAU Colloq. 161, Astronomical and Biochemical Origins and the Search for Life in the Universe*, ed. C. B. Cosmovici, S. Bowyer, & D. Werthimer, (Bologna: Editrice Compositori), 89
- . 2001, in *The Bridge Between the Big Bang and Biology*, ed. F. Giovannelli (Rome: CNR), 139
- Charnley, S. B., Ehrenfreund, P., & Kuan, Y.-J. 2001, *Spectrochim. Acta A*, 57, 685
- Charnley, S. B., Kress, M. E., Tielens, A. G. G. M., & Millar, T. J. 1995, *ApJ*, 448, 232
- Charnley, S. B., Rodgers, S. D., & Ehrenfreund, P. 2001, *A&A*, 378, 1024
- Charnley, S. B., Tielens, A. G. G. M., & Millar, T. J. 1992, *ApJ*, 399, L71
- Chyba, C. F., Thomas, P. J., Brookshaw, L., & Sagan, C. 1990, *Science*, 249, 366
- Combes, F., Nguyen-Q-Rieu, & Wlodarczak, G. 1996, *A&A*, 308, 618
- Cronin, J. R., & Chang, S. 1993, in *The Chemistry of Life's Origins*, ed. J. M. Greenberg, C. X. Mendoza-Gómez, & V. Pirronello (NATO ASI Ser. C, 416; Dordrecht: Kluwer), 209
- Császár, A. G. 1992, *J. Am. Chem. Soc.*, 114, 9568
- Cummins, S. E., Linke, R. A., & Thaddeus, P. 1986, *ApJS*, 60, 819
- Delsemme, A. 1993, *Adv. Space Res.*, 15, 49
- Ehrenfreund, P., Bernstein, M. P., Dworkin, J. P., Sandford, S. A., & Allamandola, L. J. 2001a, *ApJ*, 550, L95
- Ehrenfreund, P., & Charnley, S. B. 2000, *ARA&A*, 38, 427
- Ehrenfreund, P., d'Hendecourt, L. B., Charnley, S. B., & Ruiterkamp, R. 2001b, *J. Geophys. Res.*, 106, 33291
- Ehrenfreund, P., Glavin, D. P., Botta, O., Cooper, G. W., & Bada, J. L. 2001c, *Proc. Natl. Acad. Sci.*, 98, 2138
- Ehrenfreund, P., & Schutte, W. A. 2000, in *IAU Symp. 197, Astrochemistry: From Molecular Clouds to Planetary Systems*, ed. Y. C. Minh & E. F. van Dishoeck (San Francisco: ASP), 135
- Gibb, E. L., et al. 2000, *ApJ*, 536, 347
- Guélin, M., & Cernicharo, J. 1989, in *Physics and Chemistry of Interstellar Molecular Clouds*, ed. G. Winnenwiser & T. Armstrong (Berlin: Springer), 337
- Halfen, D. T., Apponi, A. J., & Ziurys, L. M. 2001, *ApJ*, 561, 244
- Helo, E. 2003, in *IAU Symp. 213, Bioastronomy 2002: Life among the Stars*, in press
- Hollis, J. M., Lovas, F. J., Jewell, P. R., & Coudert, L. H. 2002, *ApJ*, 571, L59
- Hollis, J. M., Snyder, L. E., Suenram, R. D., & Lovas, F. J. 1980, *ApJ*, 241, 1001
- Hollis, J. M., Vogel, S. N., Snyder, L. E., Jewell, P. R., & Lovas, F. J. 2001, *ApJ*, 554, L81
- Hunt, M. R., et al. 2003, in *IAU Symp. 213, Bioastronomy 2002: Life among the Stars*, in press
- Ikeda, M., Ohishi, M., Nummelin, A., Dickens, J. E., Bergman, P., Hjalmarsen, A., & Irvine, W. M. 2001, *ApJ*, 560, 792
- Jaffe, D. T., Becklin, E. E., & Hildebrand, R. H. 1984, *ApJ*, 279, L51
- Karpas, Z., & Mautner, M. 1989, *J. Phys. Chem.*, 93, 1859
- Kuan, Y.-J., Pen, M.-L., Huang, H.-C., Veal, J. M., & Woodney, L. M. 2003a, in *IAU Symp. 213, Bioastronomy 2002: Life among the Stars*, in press
- Kuan, Y.-J., & Snyder, L. E. 1994, *ApJS*, 94, 651
- . 1996, *ApJ*, 470, 981
- Kuan, Y.-J., et al. 2003b, in *IAU Symp. 213, Bioastronomy 2002: Life among the Stars*, in press
- . 2003c, in *12th Rencontres de Blois, Frontiers of Life*, in press
- Lee, C. W., Cho, S.-H., & Lee, S.-M. 2001, *ApJ*, 551, 333
- Liu, S.-Y., Girart, J. M., Remijan, A., & Snyder, L. E. 2002, *ApJ*, 576, 255
- Liu, S.-Y., Mehringer, D. M., & Snyder, L. E. 2001, *ApJ*, 552, 654
- Lovas, F. J., Kawashima, Y., Grabow, J.-U., Suenram, R. D., Fraser, G. T., & Hirota, E. 1995, *ApJ*, 455, L201
- Mehring, D. M., Snyder, L. E., Miao, Y., & Lovas, F. J. 1997, *ApJ*, 480, L71
- Miao, Y., Snyder, L. E., Kuan, Y.-J., & Lovas, F. J. 1994, *BAAS*, 26, 906
- Miller, S. L. 1957, *Biochem. Biophys. Acta.*, 23, 480
- Muñoz-Caro, G. M., et al. 2002, *Nature*, 416, 403
- Nummelin, A., Bergman, P., Hjalmarsen, A., Freberg, P., Irvine, W. M., Millar, T. J., Ohishi, M., & Saito, S. 2000, *ApJS*, 128, 213
- Ohishi, M., Ishikawa, S.-I., Yamamoto, S., Saito, S., & Amano, T. 1995, *ApJ*, 446, L43
- Oró, J. 1961, *Nature*, 190, 389
- Pickett, H. M., Poynter, R. L., Cohen, E. A., Delitsky, M. L., Pearson, J. C., & Müller, H. S. P. 1998, *J. Quant. Spectrosc. Radiat. Transfer*, 60, 883
- Remijan, A., Snyder, L. E., Liu, S.-Y., Mehringer, D., & Kuan, Y.-J. 2002, *ApJ*, 576, 264
- Snyder, L. E. 1997, *Origins Life Evol. Biosphere*, 27, 115
- Snyder, L. E., Hollis, J. M., Suenram, R. D., Lovas, F. J., Brown, L. W., & Buhl, D. 1983, *ApJ*, 268, 123
- Sorrell, W. H. 2001, *ApJ*, 555, L129
- Suenram, R. D., & Lovas, F. J. 1978, *J. Mol. Spectrosc.*, 72, 372
- . 1980, *J. Am. Chem. Soc.*, 102, 7180
- Sutton, E. C., Blake, G. A., Masson, C. R., & Phillips, T. G. 1985, *ApJS*, 58, 341
- Sutton, E. C., Peng, R., Danchi, W. C., Jaminet, P. A., Sandell, G., & Russell, A. P. G. 1995, *ApJS*, 97, 455
- Turner, B. E. 1989, *ApJS*, 70, 539
- . 1991, *ApJS*, 76, 617
- Turner, B. E., & Apponi, A. J. 2001, *ApJ*, 561, L207
- Wright, M. C. H., Plambeck, R. L., & Wilner, D. J. 1996, *ApJ*, 469, 216
- Zhang, Q., Ho, P. T. P., & Ohashi, N. 1998, *ApJ*, 494, 636